First publ. in: Journal of Physics: Condensed Matter 4 (1992), pp. 7709-7744

A theory for the β-relaxation process near the liquid-to-glass crossover

M Fuchs, W Götze†, S Hildebrand and A Latz

Physik Department, Technische Universität München, D-8046 Garching, Federal Republic of Germany

Received 6 April 1992, in final form 12 June 1992

Abstract. The mode coupling theory for supercooled liquid dynamics finds a β-relaxation regime on mesoscopic timescales. It is caused by the interplay between nonlinear interactions of density fluctuations and phonon-assisted hopping transport. In this regime all correlation functions and spectra can be expressed in terms of a single β-correlator G, which is a homogeneous function of time and two relevant control parameters. It is specified by a single number, namely the exponent parameter λ. Eight regions can be identified, where the equation for G can be solved by series expansions. The various possibilities are discussed in comparison with representative numerical solutions. For temperatures T sufficiently above the critical value T_c hopping effects can be neglected and a stretched susceptibility minimum is found as a crossover from von Schweidler decay to critical decay. For T near T_c hopping effects balance the cage effect and this results on logarithmic scales in a rather abrupt crossover from the high-frequency α-peak tail to the critical spectrum. For T below T_c there appears a frequency window between two knees in the susceptibility spectrum, where hopping effects suppress the enhanced fractal spectra. There occurs a crossover from Debye relaxation to white noise. The resulting susceptibility minimum in the strongly supercooled state exhibits a subtle power law dependence on the separation parameter $T - T_c$. The measurable features in the susceptibility, such as position and strength of the minimum, are evaluated and shown to characterize transparently the liquid-to-glass crossover as caused by the underlying glass transition singularity.

1. Introduction

The most prominent features of glassy relaxation in cooled liquids are the low-lying susceptibility bumps, called α peaks. The timescale τ_α of the α process increases dramatically upon cooling. For a temperature T near the melting point τ_α is somewhat larger than the time t_0 specifying the dynamics of microscopic excitations such as phonons. If T approaches the calorimetric glass transition value T_g, the scale τ_α is of macroscopic size. There are also subtle dynamical phenomena, referred to as β processes. They are observed within the mesoscopic window for the time t, $\tau_\alpha \gg t \gg t_0$; they can be measured as spectra for the frequency ω within the window $\tau_\alpha^{-1} \ll \omega \ll t_0^{-1}$ [1]. Goldstein argued convincingly [2] that an understanding of the β process is the key for a microscopic explanation of the liquid-to-glass crossover in

† Also at Max Planck Institut für Physik (Werner Heisenberg Institut), PO Box 401212, D-8000 München, Federal Republic of Germany.

simple systems. In recent years the mode coupling theory (MCT) for the dynamics of cooled liquids has been discussed, which obtains α and β processes resembling the experimental results for fragile glass formers. For an overview the reader may consult [3] and a review of the mathematical details can be found in [4]. In this paper the previous work shall be extended to a complete discussion of the MCT results for the β process.

The MCT derives from closed equations of motion conventionally defined autocorrelation functions $\Phi_X(t)$ for dynamical variables X [5]. The variables X of interest are the density fluctuations ρ_q of wavevector q, the dipole moment D, the stress π, a coupling variable to photons $\sum_{kp} C_{q,kp}\rho_k\rho_p$ consisting of superpositions of density fluctuation pairs, and so on. In these examples $\Phi_X(t)$ can respectively be measured by neutron scattering, by dielectric loss spectroscopy, by acoustic spectroscopy or conventional Brillouin scattering experiments, and by depolarized light-scattering or second-order Raman scattering. The MCT equations are regular; the mathematical control-parameter, a vector V in some high-dimensional parameter space $\mathcal{K}$, depends smoothly on the physical control parameters such as temperature T or density n. However, the equations bring out a spontaneous singularity V_c, called the glass transition singularity, by means of a Whitney fold bifurcation [4]. This bifurcation implies slow and stretched relaxation processes. There appears a small parameter, namely the distance from the singularity, permitting analytic asymptotic solutions of the complicated equations of motion. These asymptotic solutions comprise the essential qualitative features of the MCT. It was proposed to test whether they also reflect the qualitative features of the experiments. Only if this were the case would one shoulder the burden and solve the MCT equations in quantitative detail.

For β relaxation the MCT predicts some universality features. One is the factorization property:

$$\Phi_X(t) - f_X^c = h_X G(t). \tag{1.1a}$$

Here $f_X^c > 0$ is the Edwards–Anderson parameter, or non-ergodicity parameter, at the singularity and $h_X \geqslant 0$ is called the critical amplitude. These time-independent quantities are determined by the equilibrium structure of the system and they contain all microscopic specifications of X. The time and the sensitive temperature dependence enter via the β-correlator G, which is the same for all variables X of a given system. Let us mention in passing that the β-relaxation regime is defined implicitly by requiring $|h_X G(t)/f_X^c| \ll 1$. Within the β region, the correlator Φ_X is close to arrest near f_X^c. For a precise definition see equation (2.5) below. Spectra are denoted as usual by $\Phi_X''(\omega)$, $G''(\omega)$ and they are defined as Fourier cosine transforms of the corresponding correlator. The susceptibilities $\chi(\omega) = \chi'(\omega) + i\chi''(\omega)$ are related to the Laplace transform of the correlator $\Phi(z) = \mathcal{LT}[\Phi(t)](z)$, $z = \omega + i0$, by $\chi_X(\omega) = z\Phi_X(\omega) + \chi_X^0$. Here χ_X^0 is the thermodynamic susceptibility and the following convention is used: $\mathcal{LT}[\Phi(t)] = i\int dt\,\Theta(t)\exp(izt)\Phi(t)$ [5]. One gets as an equivalent to (1.1a) the factorization

$$\chi''(\omega) = h_X\chi''(\omega) \qquad \chi'(\omega) - \chi_X^c = h_X\chi'(\omega). \tag{1.1b}$$

Now $\chi''(\omega) = \omega G''(\omega)$ denotes the β-susceptibility spectrum. Similarly, the relations $\chi'(\omega) = \omega G'(\omega)$ and $\chi_X^c = \chi_X^0 - f_X^c$ hold. Thus up to constants h_X all spectra

are the same function $\chi''(\omega)$. This is valid not only for the dependence on frequency but also for the singular dependence of the spectra on control parameters such as T.

The second universality feature concerns the β correlator itself, which is fixed by the four numbers t_0, λ, σ and δ. The timescale t_0 connects mathematical time with physical time. The exponent parameter λ, obeying $1/2 \leqslant \lambda < 1$, specifies the details of the dynamics near V_c. It fixes three characteristic exponents describing fractal decay patterns. The critical exponent a, obeying $0 < a \leqslant 0.395\ldots$, follows from

$$\frac{\Gamma(1-a)^2}{\Gamma(1-2a)} = \lambda \tag{1.2a}$$

and the von Schweidler exponent b, obeying $0 < b \leqslant 1$, is obtained from

$$\frac{\Gamma(1+b)^2}{\Gamma(1+2b)} = \lambda. \tag{1.2b}$$

These exponents decrease monotonically to zero if λ increases towards unity. For $\lambda = \pi/4$ one finds, for example, $a = 0.287\ldots$, $b = 0.500$. It will be shown that for $\lambda > \pi/4$ a further exponent c is relevant. It obeys $0 < c < 0.5$, decreases to zero if λ tends to unity, and follows from

$$\frac{\Gamma(\frac{3}{2})\Gamma(1+c)}{\Gamma(\frac{3}{2}+c)} = \lambda. \tag{1.2c}$$

Throughout this paper Γ denotes the gamma function. The quantities (σ, δ) are the relevant control parameters. The glass transition singularity is specified by $\sigma = 0$, $\delta = 0$. Both parameters depend smoothly on physical control parameters such as T. The zero of σ defines critical control parameters such as T_c. For example, one can write

$$\sigma = C\frac{T_c - T}{T_c} \tag{1.3}$$

where $C > 0$ for T near T_c. The parameter σ is called the separation parameter. It is given by the equilibrium structure of the system, as is λ. These two parameters specify the cage effect of liquid dynamics. They are the same, for instance, for a hard-sphere system obeying Newtonian dynamics and one following Brownian dynamics. It is the potential landscape in phase space that governs the cage statistics and self-blocking events. Details of the microscopic motion enter merely via the scale t_0, specifying the speed with which the particles explore the landscape. Within the so-called simple version of the MCT, dealing with the cage effect only, a transition from ergodic motion for $\sigma < 0$ to non-ergodic dynamics for $\sigma > 0$ is found. The ideal glass is characterized by $\Phi_X(t \to \infty) = f_X > 0$, i.e. by an extensive number of degenerate metastable states [6]. Since there are no long-range correlations within a glass, the activation barriers between the metastable states are finite. The parameter $\delta > 0$ describes the rate for phonon-assisted hopping events from one state to the other. These hopping events restore ergodicity for all σ. The hopping parameter depends on the microscopic details of the dynamics and will be quite different for a hard sphere system in a vacuum on the one hand, and a hard spherical colloidal suspension on the other hand. One gets

$$G(t) = g^{\lambda}(t/t_0, \sigma, \delta t_0). \tag{1.4}$$

We will not indicate explicitly in the following that the function of three variables g^λ is determined by λ.

Within the MCT it is important to treat wavevector dependencies properly in the equations of motion. This is particularly essential if one wants to understand the T dependence of the hopping rate δ [7]. It is a non-trivial result that within the β regime all these detailed complications can be condensed to the two numbers σ, δ. The formulated results (1.1) and (1.4) hold only in leading order for $(\sigma, \delta) \to (0,0)$, see equation (2.5). There are corrections to the asymptotic results and these are not universal. The range of validity of (1.1) and (1.4) may be different for different X and the deviations cannot be specified by σ and δ alone. In leading order the quantities h_X, C, t_0 and δ have to be replaced by their values for $T = T_c$ so that the T dependence only enters via σ. For practical applications, however, the MCT results have been used for $|T - T_c|$ as large as 100 degrees. In those cases one has to allow a smooth T dependence of h_X, t_0 and δ.

So far the quantitative effect of hopping on the correlator G has been discussed only within a schematic model [8]. Adjusting constants so that the α spectrum agreed within an order of magnitude with the dielectric loss curves for the standard glass former $CaKNO_3$ (CKN) it was found that $\delta t_0 \sim 10^{-6}$ and δt_0 decreased by between one to two orders of magnitude upon lowering T through T_c. The relevance of these findings for the β-relaxation theory is not obvious at present, but in the following we will consider them as educated guesses for the size of the hopping effects.

Previous comparisons of experiments with MCT results have been restricted to the simple version, where the hopping effects are ignored. In this case the β correlator obeys a one-parameter scaling law:

$$G(t) = c_\sigma g_\pm (t/t_\sigma) \qquad \sigma \gtrless 0 \qquad \delta = 0. \tag{1.5}$$

The correlation scale c_σ vanishes and the timescale t_σ diverges at the critical point, $c_\sigma = |\sigma|^{1/2}$, $t_\sigma = t_0 |\sigma|^{-1/2a}$. The master functions $g_\pm$, given by λ, can be evaluated easily [9]. For short rescaled times $\hat{t} = t/t_\sigma$, one finds critical decay

$$g_\pm(\hat{t} \ll 1) = \frac{1}{\hat{t}^a}. \tag{1.6}$$

For larger rescaled times the glass correlator arrests:

$$g_+(\hat{t} \gg 1) = \frac{1}{\sqrt{1-\lambda}}. \tag{1.7a}$$

This means that the correlator gets a contribution from the Edwards–Anderson parameter, which shows a cusp singularity at the critical point:

$$G(t) \to \chi_\infty = \sqrt{\frac{\sigma}{1-\lambda}} \qquad \sigma > 0 \qquad \frac{t}{t_\sigma} \to \infty \qquad \delta = 0. \tag{1.7b}$$

On the liquid side of the transition, the correlator obeys the von Schweidler law:

$$g_-(\hat{t} \gg 1) = -B^- \hat{t}^b. \tag{1.8}$$

Here $B^- > 0$ is of order unity [9]. Notice that the fractal decay laws (1.6) and (1.8) appear, even though no fractal structures in configuration space are built into the MCT

equations of motion. The power laws result from the interplay of retardation effects and nonlinearities. Let us notice for later reference that a power law correlator

$$G(t) = (\tau/t)^x \tag{1.9a}$$

implies for the susceptibility similar power laws:

$$\omega G''(\omega) = \sin(\pi/2x)\,\Gamma(1-x)(\omega\tau)^x \tag{1.9b}$$

$$\omega G'(\omega) = -\cos(\pi/2x)\,\Gamma(1-x)(\omega\tau)^x. \tag{1.9c}$$

The role of the hopping effect in its interplay with the cage effect is exhibited most clearly for vanishing separation parameter. In this case one finds a one-parameter scaling law quite similar to (1.5) [10]:

$$G(t) = c_\delta g(t/t_\delta) \qquad \sigma = 0. \tag{1.10}$$

The master function g is independent of δ and given by λ. The scales are again determined by the exponent a: $c_\delta = (\delta t_0)^{a/(1+2a)}$, $t_\delta = t_0(\delta t_0)^{-1/(1+2a)}$. As above, critical decay is obtained for short rescaled times $g(\hat{t} \ll 1) = 1/\hat{t}^a$. For large times, however, there are two possibilities, depending on the sign of

$$\Delta\lambda = \lambda - \lambda_0 \qquad \lambda_0 = \frac{\pi}{4}. \tag{1.11}$$

For exponent parameters smaller than the critical value λ_0, one again finds the von Schweidler law (1.8)

$$g(\hat{t} \gg 1) = -B\hat{t}^b \qquad b > \tfrac{1}{2}. \tag{1.12a}$$

However for $\Delta\lambda > 0$ a von Schweidler law with universal exponent 1/2 is obtained:

$$g(\hat{t} \gg 1) = -(\Delta\lambda)^{-1/2}\hat{t}^{1/2} \qquad b < \tfrac{1}{2}. \tag{1.12b}$$

One motivation of this paper is to investigate the susceptibility spectra implied by the master function g and to understand the relaxation for $\Delta\lambda = 0$.

Neutron scattering experiments done for CKN [11], orthoterphenyl [12], polybutadien [13] and propylene carbonate [14] provided some support of the MCT, as can also be inferred from the work quoted in the mentioned papers. The validity of the scaling laws (1.5), the validity of the master function g_- and the scale variations with σ have been successfully tested against experiments for polymer dielectric loss spectra [15, 16], for neutron scattering cross sections of a biopolymer [17], for photon correlation curves for a colloidal suspension [18, 19] and for correlators obtained by molecular dynamics work for a model liquid [20, 21]. All those mentioned papers deal with the weak coupling side $\sigma < 0$ of the transition. Extensive tests of (1.5)–(1.8) have been carried out recently for $\sigma > 0$ and $\sigma < 0$ with depolarized light-scattering spectra, done within a four-decade frequency window for CKN, by Cummins, Li and collaborators [22, 23]. The theory accounted for the data within the large temperature interval 23° C $< T <$ 195° C. The critical point was identified as $T_c = (105 \pm 5)$° C in accord with results obtained from neutron scattering spectroscopy [24]. Even though the applicability of the MCT is still highly controversial [25], the above-mentioned

quantitative confirmations of that theory appear as a sufficient justification to continue with this approach.

For $T - T_c$ as large as 90° C the CKN light-scattering data [22, 23] demonstrate a merging of the α–β relaxation spectra with the microscopic excitation band, as expected from MCT model calculations [8]. For such large $(T - T_c)$ the asymptotic formulae, based on the $\sigma \to 0$ limit, can no longer be used for a quantitative data analysis. However, the light-scattering spectra for CKN [22, 23] also show systematic deviations from the β-relaxation results of the simple MCT version (1.5) for T near T_c. These deviations are suspected to be caused by hopping effects, described by $\delta \neq 0$. This observation provides the main motivation of the present paper, where the complete β correlator (1.4), in particular the properties caused by $\delta \neq 0$, shall be discussed in all details. It is hoped that the results of the following calculations can serve as the basis of future quantitative tests for the MCT predictions on the interplay between ergodicity-breaking cage effects and ergodicity-restoring hopping events.

2. Basic formulae

The following analysis is based on the equation derived by Götze and Sjögren [10] for the β correlator:

$$-\sigma + \frac{i\delta}{z} + \lambda z \mathcal{LT}[G(t)^2](z) + (z\mathcal{LT}[G(t)](z))^2 = 0. \tag{2.1}$$

The derivation of (2.1) is based on a leading asymptotic solution of the MCT equations of motion near a glass transition singularity, as specified below in (2.5). The MCT equations in turn are obtained within the generalized kinetic equation approach towards liquid dynamics, combined with Kawasaki's factorization approximations; compare [4] for details.

It is more convenient to rewrite this scaling equation in a form that avoids Laplace transforms [9]:

$$\sigma - \delta t + \lambda G(t)^2 = \frac{d}{dt} \int_0^t G(t - t')G(t')\,dt'. \tag{2.2}$$

It has to be complemented by the initial condition

$$\lim_{t \to 0} \frac{G(t)}{G_{cr}(t)} = 1 \qquad G_{cr}(t) = \left(\frac{t_0}{t}\right)^a. \tag{2.3}$$

The critical decay G_{cr} is the dynamical signature of the underlying fold singularity. At the transition $(\sigma, \delta) = (0, 0)$ it describes the long-time behaviour of the full MCT equations.

For a numerical determination of G, equation (2.2) was discretized as done previously for $\delta = 0$ [9]. To get results for dynamical ranges as large as 15 decades, the step size for the time grid was allowed to expand with increasing t. Roughly, equally spaced time points were chosen on a logarithmic scale. A similar grid was applied to evaluate the Fourier transforms with a Filon procedure.

The correlator G obeys a two-parameter scaling law [10]. A scaling line in the σ–δt_0 parameter half-plane, $\delta \geqslant 0$, shall be defined by

$$\sigma = \hat{\sigma}\Omega^{2a} \qquad \delta t_0 = \hat{\delta}\Omega^{1+2a}. \tag{2.4a}$$

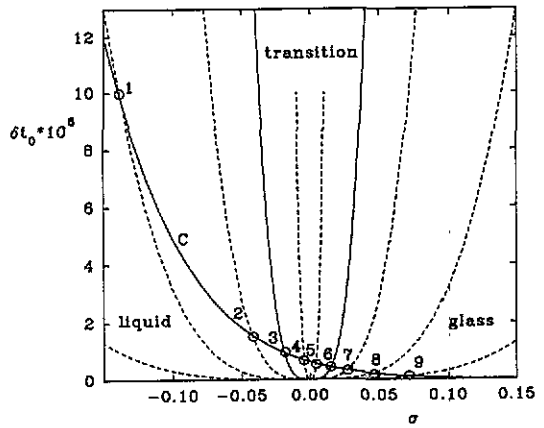

Figure 1. The control parameter half-plane with scaling lines (2.4*a*) for the exponent parameter $\lambda = 0.91$. The full scaling lines through the points 3 and 6 are the ones with $\sigma = \mp\sigma_0$, equation (3.2). The points 1–9 where the path C intersects the scaling lines have the following coordinates $(\sigma 10^2, \delta t_0 10^6) = (-14, 10)$, $(-4.2, 1.53)$, $(-1.9, 1.0)$, $(-0.47, 0.70)$, $(0.44, 0.57)$, $(1.5, 0.44)$, $(2.7, 0.33)$, $(4.6, 0.21)$, $(7.0, 0.09)$; see text.

Here the dimensionless frequency Ω is the line parameter. For $\Omega \to 0$ the line approaches the glass transition singularity. If the time is rescaled as

$$t = \frac{\hat{t} t_0}{\Omega} \tag{2.4b}$$

the correlator (1.4) merely changes its scale:

$$g(t/t_0, \sigma, \delta t_0) = c_\Omega g\left(\hat{t}, \hat{\sigma}, \hat{\delta}\right) \qquad c_\Omega = \Omega^a. \tag{2.4c}$$

The correlator is a generalized homogeneous function of the three variables t/t_0, σ, δ. Moving the parameter pair (σ, δ) along a scaling line (2.4*a*), G merely changes in a self-similar manner. It is sufficient to evaluate the correlator $\hat{G}(\hat{t}) = g(\hat{t}, \hat{\sigma}, \hat{\delta})$ for the point $(\hat{\sigma}, \hat{\delta})$, in order to know G for all points (σ, δ) on the scaling line through $(\hat{\sigma}, \hat{\delta})$. Similarly one gets for the susceptibility

$$\chi(z) = c_\Omega \hat{\chi}(\hat{z}) \qquad z = \Omega \frac{\hat{z}}{t_0} \tag{2.4d}$$

where $\hat{\chi}$ is the susceptibility corresponding to $\hat{G}(\hat{t})$ evaluated for $(\hat{\sigma}, \hat{\delta})$. Thus, in a double-logarithmic presentation of the susceptibility spectra, the graphs $\log \chi''$ against $\log \omega$ referring to different points on the scaling line have the same shape. They are created from the spectrum for $(\hat{\sigma}, \hat{\delta})$ by a shift $\log \Omega$ parallel to the $\log \omega$ axis and by a shift $\log c_\Omega$ parallel to the $\log \chi''$ axis. Figure 1 exhibits the parameter half-plane with some representative scaling lines. For the simplified MCT, dealing with $\delta = 0$, only two scaling lines are involved. The half-axis $\sigma < 0$ deals with the liquid states and one can choose $\hat{\sigma} = -1$. The half-axis $\sigma > 0$ corresponds to the ideal glass states and one can take $\hat{\sigma} = +1$. With (1.5) one gets $g_\pm(\hat{t}) = g(\hat{t}, \pm 1, 0)$. Our numerical solution of (2.2) has been done with $\hat{\sigma} = \pm 1$, also. The result for $\sigma \to 0$ was obtained in the limit $\hat{\delta} \to \infty$.

The scaling law allows for a precise mathematical definition of the β-relaxation regime. Consider a path $\Omega \to V(\Omega)$ in control parameter space K. The theory of the bifurcation singularity maps that path onto one in the σ–δt_0 plane: $\Omega \to (\sigma(\Omega), \delta(\Omega))$. Assume the latter to be a scaling line so that in particular $V(\Omega \to 0) \to V_c$. The correlators will vary in a complicated manner with Ω, as defined by the solution of the full MCT equations of motion: $\Phi_X(t) = \Phi_X^\Omega(t)$. But in the limit of small Ω one finds

$$\lim_{\Omega \to 0} \frac{\Phi_X^\Omega(t) - f_X^c}{c_\Omega} = h_X \hat{G}(\hat{t}). \tag{2.5}$$

If V moves towards V_c on a line $V(\Omega)$, the RHS of (1.1a) vanishes in proportion to c_Ω, provided the time increases towards infinity as given by (2.4b). The corrections to (1.1a), $\Phi_X(t) - f_X^c - h_X G(t)$, vanish in proportion to c_Ω^2. Let us emphasize the following: within the MCT neither an ansatz nor a scaling assumption is introduced in order to obtain the results (1.1), (1.4), (2.1) and (2.5). These formulae are mathematical implications of the existence of a bifurcation singularity of the Whitney fold type. They reflect the centre manifold theorem of singularity theory. The existence of a bifurcation singularity for the infinite set of equations of motion of the MCT, derived for density and current density fluctuations for simple classical liquids, has been proven previously; compare [4] and the original references quoted therein.

A full test of the MCT would require us to map out experimentally the two-dimensional half-plane of relevant control parameters $(\sigma, \delta t_0)$, shown in figure 1. In particular one should move on scaling lines in order to test the homogeneity (2.4) and approach the singularity very closely in order to eliminate the corrections to the leading-order results (1.1) and (1.4). The problem is familiar from ordinary phase transition theories in finite systems. The present δ is the analogue of the inverse box diameter $1/L$. For ordinary phase transitions one can vary σ and $1/L$ and extrapolate, e.g., to $1/L \to 0$. The MCT of the liquid-to-glass crossover is more complicated to understand, because δ cannot be manipulated and extrapolation to $\delta \to 0$ can be considered as a theoretical idealization only. The MCT equations determine V in terms of the physical control parameters, say T. Thus the system moves on a path C: $T \to (\sigma(T), \delta(T))$ as sketched in figure 1 by a curve through the points 1 to 9. This path is fixed by the microscopic details of the given system and cannot be varied. In particular, C avoids the singularity [10]. All functions vary smoothly with T. There is no sharp transition for $T = T_c$. But passing from $T > T_c$ to $T < T_c$, the dynamics alters drastically. This is exemplified in figure 2, showing the evolution of the susceptibility spectra along C from figure 1. For example, for state 2 the spectrum exhibits a broad minimum connected with a crossover from some fractal decrease to some fractal increase with increasing frequency. But state 6 has a much sharper minimum and on both sides of the latter there are knees in the $\log \chi''$ against $\log \omega$ curves. The knees and the minima scale differently with changes of σ.

3. The various relaxation regimes

3.1. The β-relaxation scales

In this section eight regions will be identified in the three-dimensional manifold of variables $(t/t_0, \sigma, \delta t_0)$, where $G(t)$ can be evaluated analytically as a power

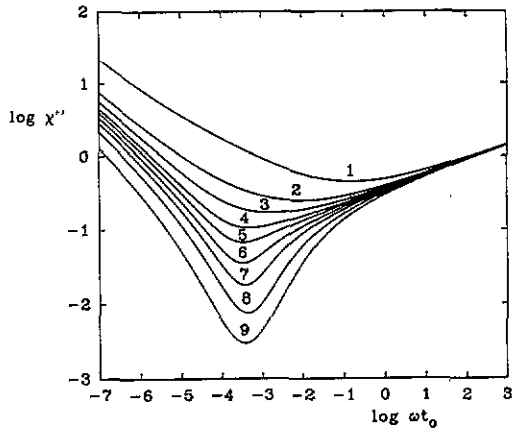

Figure 2. Susceptibility spectra for $\lambda = 0.91$ and the parameter points 1–9 specified in figure 1.

series. Within these regions the β correlator can be understood qualitatively as the leading contribution to the respective series. A complete qualitative understanding of the solution of (2.2) is achieved by interpolation between the series referring to neighbouring regions. The various regimes are separated by surfaces, which can be described by $t = t_{sc}(\sigma, \delta t_0)$. There appear five such functions t_{sc}; they are the relevant timescales for the β dynamics. Because of (2.4) they are homogeneous functions of the control parameters:

$$t_{sc}(\sigma, \delta t_0) = \Omega^{-1} t_{sc}(\sigma\Omega^{-2a}, \delta t_0 \Omega^{-(1+2a)}). \tag{3.1}$$

It is sufficient to know the scale $\hat{t}_{sc} = t_{sc}(\hat{\sigma}, \hat{\delta})$ for one pair $(\hat{\sigma}, \hat{\delta})$ in order to know it on the complete scaling line through that pair. Due to the scaling law it is sufficient to consider a representative cut through the $(t/t_0, \sigma, \delta t_0)$ manifold; the surfaces $t = t_{sc}(\sigma, \delta t_0)$ yield curves on this cut. Figure 3 exhibits the cut $\delta t_0 = 1$ for a representative critical exponent $a = 0.200$.

Let us consider (3.1) with $\Omega = |\sigma|^{1/2a}$. One gets for $\sigma \gtrless 0$

$$t_{sc} = t_{sc}(\pm 1, (|\sigma|/\sigma_0)^{-(1+2a)/2a}) |\sigma|^{-1/2a}$$

where

$$\sigma_0 = (\delta t_0)^{2a/(1+2a)}. \tag{3.2}$$

If $t_{sc}(\pm 1, x)$ depends smoothly on x for small x, one gets $t_{sc} \approx t_{sc}(\pm 1, 0)|\sigma|^{-1/2a}$ for $|\sigma_0/\sigma| \ll 1$. Thus one identifies the scales

$$c_\sigma = |\sigma|^{1/2} \qquad t_\sigma = t_0 |\sigma|^{-1/2a} \tag{3.3}$$

as relevant for a sufficiently large separation parameter. This is the only scale that enters the simple version of the MCT, leading to (1.5).

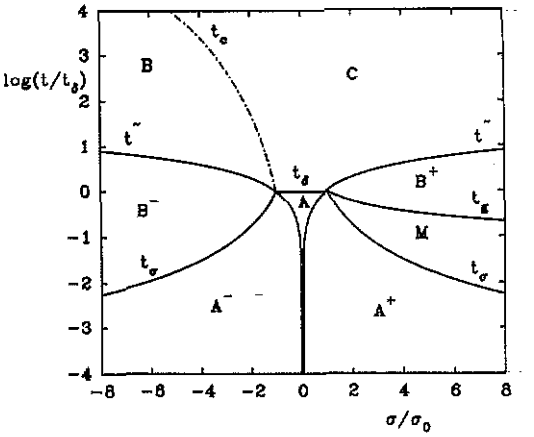

Figure 3. Various dynamical regions $A^-, A, A^+, B^-, B, B^+, C$ and M separated by the timescales $t_\sigma, t_\delta, \tilde{t}, t_g$ and t_c for $\lambda = 0.91$ as defined in the text.

Let us apply (3.1) with $\Omega = (\delta t_0)^{1/(1+2a)}$ leading to

$$t_{sc} = t_{sc}(\sigma/\sigma_0, 1)(\delta t_0)^{-1/(1+2a)}.$$

If again $t_{sc}(x,1)$ depends smoothly on x for $x \to 0$, one gets $t_{sc} \approx t_{sc}(0,1)(\delta t_0)^{-1/(1+2a)}$ for $|\sigma| \ll \sigma_0$. Thus one identifies the scales entering (1.10)

$$c_\delta = (\delta t_0)^{a/(1+2a)} \qquad t_\delta = t_0(\delta t_0)^{-1/(1+2a)} \tag{3.4}$$

as relevant for small separation parameter. The hopping rate introduces σ_0 as the natural scale for the separation parameter [10].

Below it will be shown in detail that the relaxation patterns are pairwise quite different for the three cases: the liquid region $\sigma \ll -\sigma_0$, the transition region $|\sigma| \ll \sigma_0$ and the glass region $\sigma \gg \sigma_0$. The spectra in figure 2, where 1 and 2 refer to the liquid, 4 and 5 to the transition region, and 8 and 9 to the glass, exemplify this statement. For the characteristic separation $\pm\sigma_0$, hopping effects and cage effects are of equal importance for the β dynamics if $t \approx t_\sigma \approx t_\delta$.

A natural scale $\tilde{t}$ appears, if one compares the cage effect term and the hopping term as they enter the scaling equation (2.1) or (2.2) [10]:

$$\tilde{t} = |\sigma|/\delta = \Omega^{-1}|\hat{\sigma}|/\hat{\delta}. \tag{3.5}$$

From $\tilde{t}$ and t_σ one gets a further scale as the geometric mean

$$t_g = (\tilde{t}t_\sigma)^{1/2} = t_0/(\delta t_0|\sigma|^{(1-2a)/2a})^{1/2}. \tag{3.6}$$

This scale will be relevant for the glass only. Finally there will enter a scale t_c, specifying a crossover in the liquid state

$$t_c = \tilde{t}\,(\tilde{t}/t_\sigma)^{2b/(1-2b)}. \tag{3.7}$$

The scale t_c is only relevant if $b < 1/2$ is fulfilled; it is shown as the chain curve in figure 3. The value $b = 1/2$ plays a distinguished role for the hopping-controlled relaxation for very long times.

The various β-relaxation results are demonstrated in figures 4–9. For the three regions $\sigma \ll -\sigma_0$, $|\sigma| \ll \sigma_0$ and $\sigma \gg \sigma_0$ two representative exponent parameters are considered: $\lambda = 0.74 < \lambda_0$ is connected with exponents $a = 0.31$, $b = 0.58$ and $\lambda = 0.91 > \lambda_0$ leads to $a = 0.20$, $b = 0.28$ and $c = 0.17$. The full curves exhibit the numerical solution of (2.2). The various series expansions are shown as broken curves; they carry labels such as A, B^-, and so on, referring to the respective series such as (3.13) and (3.15), where the coefficients are denoted by A_l, B_l^- etc. A similar labeling is done in figure 3 to indicate the relevant regions, where the series can be used. The recursion relations for the series coefficients are derived in appendix A and referred to by equation numbers like (A6) or (A9).

Let us re-emphasize that the correlator $G(t)$ or the spectrum $G''(\omega)$ change smoothly with σ and δ. The solutions of (2.2) do not exhibit singularities of any kind, since the glass transition singularity is avoided, which means $\delta(T = T_c) > 0$. Therefore concepts such as liquid, transition region and glass, or the relaxation regimes A, B^-, and so on, are fuzzy. The definition of the scales is to some extent arbitrary; all of them can be altered by factors of order unity. The following series expansions usually work only in the limit where the triple $(t/t_0, \sigma, \delta)$ departs arbitrarily far from the borders of the corresponding region. Expansions near the intersection of scales do not have a well defined mathematical meaning; therefore the definition of the scales themselves has no relevance near these intersection points either. Figure 3 is presented as a help only to organize the following discussion.

3.2. *Short-time dynamics*

3.2.1. Relaxation within the liquid regime. If one can ignore the hopping effect within the liquid region the critical decay law can be extended to larger times by the series

$$G(t) = c_\sigma \left(\frac{t}{t_\sigma}\right)^{-a} \left(1 + \sum_l A_l^- (t/t_\sigma)^{2la}\right) \qquad \sigma \ll -\sigma_0. \tag{3.8}$$

Here, and in the following, l sums extend over $l = 1, 2, \ldots$. The coefficients $A_l^- = (-1)^l A_l^+$ are determined by the recursion relation (A5), where

$$A_1^\pm = \pm \frac{1}{2(\Gamma(1-a)\Gamma(1+a) - \lambda)}. \tag{3.9}$$

The $A_l^\pm$ are given by λ; (3.8) is the short-time expansion of g_- in (1.5). The series (3.8) converges for $t/t_\sigma < r$; r depends strongly on λ. From $l \leqslant 170$ we estimate $r = \lim_{l\to\infty} |A_l|^{-1/2al}$, to be 8.5 for $\lambda = 0.74$ and 0.9 for $\lambda = 0.91$; r tends to zero for $\lambda \to 1$.

The deviations of $G(t)$ from the critical correlator (2.3) depend sensitively on σ. They describe the suppression of $G(t)$ below $G_{cr}(t)$ so that there appears an inflection point t_i in the $G(t)$ against $\log t$ graph. Near t_i, $G(t)$ becomes negative, as shown in figures 4(a) and 5(a). Similarly, upon decreasing ω the susceptibility spectrum gets a σ-sensitive upward bending, as shown in figures 4(b) and 5(b). In

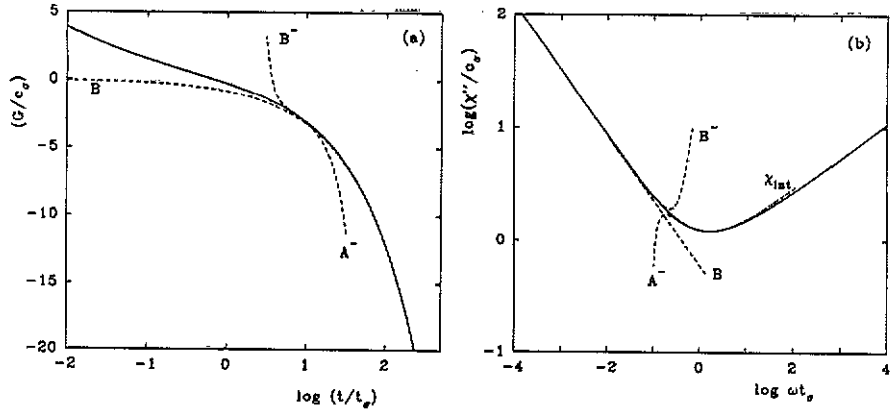

Figure 4. Correlator G as function of time t (a) and loss spectrum χ'' as function of frequency ω (b) for $\lambda = 0.74$ for a liquid state with separation parameter $\sigma/\sigma_0 = -7.2$. The broken curves are the various asymptotic expansions described in the text. The chain curve is the interpolation (3.17).

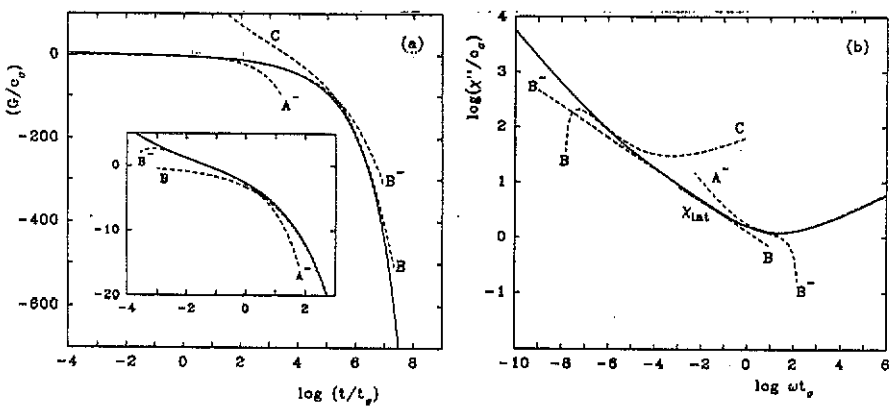

Figure 5. The same as figure 4 for $\lambda = 0.91$ and $\sigma/\sigma_0 = -7.2$.

principle, a measurement of these deviations from the critical dynamics yields σ, whose extrapolation to zero would determine T_c from the high-temperature side via equation (1.3).

The bending of the $\chi''(\omega)$ against ω curve leads to a minimum of the susceptibility spectrum at some frequency ω_{min}, where $\chi''(\omega_{min}) = \chi_{min}$. Because of (3.8) these quantities scale with the separation parameter sensitively like

$$\omega_{min} = \gamma_1^L / t_\sigma \qquad \chi_{min} = \gamma_2^L c_\sigma . \tag{3.10}$$

Here and in the following γ_1, γ_2 denote numbers, which are independent of (σ, δ) and are determined by λ. In figure 2 this scaling is the reason for the σ-dependent shift of the minimum in curve 2 relative to one in curve 1. Experimental verification of the scaling (3.10) gives a way to fix T_c from the liquid side, as can be inferred from [15, 16, 19, 21–23].

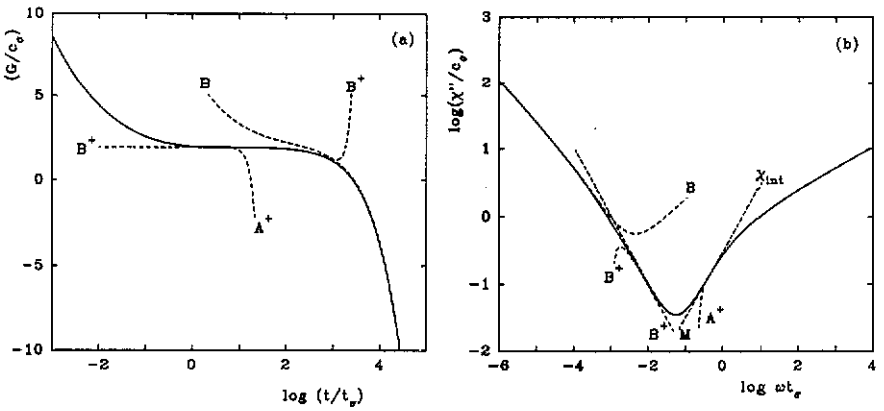

Figure 6. Correlator $G(t)$ and loss spectrum $\chi''(\omega)$ for $\lambda = 0.74$ for a glass state with $\sigma/\sigma_0 = +7.2$. The broken curves are the various series expansions described in the text and the chain curve is the interpolation formula (3.30).

3.2.2. Relaxation within the glass regime. In the glass region, where again $|\sigma|$ is large in comparison to σ_0 but now positive, one continues the critical decay as

$$G(t) = c_\sigma (t/t_\sigma)^{-a} \left(1 + \sum_l A_l^+ (t/t_\sigma)^{2la}\right) \qquad \sigma \gg \sigma_0. \tag{3.11}$$

This expression agrees with (3.8) except for changes of signs in the coefficients A_l^+ with odd values of l. The radius of convergence is the same as for the liquid. Equation (3.11) is the short-time expansion of g_+ in (1.5).

The σ-sensitive deviations from the critical decay imply an upward bending of the $G(t)$ against $\log t$ curve until the plateau value χ_∞ from (1.7*b*) is reached, as shown in figures 6(*a*) and 7(*a*). Detection of the plateau value is a means to measure σ and obtain T_c by extrapolation from the low-temperature side, as can be inferred from [12, 13, 24]. The σ-sensitive corrections to the critical spectrum suppress the $\log \chi''$ against $\log \omega$ curve below the latter one. Thus a knee is formed at some frequency ω_K where $\chi''(\omega_K) = \chi_K$. These spectral features scale with the separation parameter as

$$\omega_K = \gamma_1^K / t_\sigma \qquad \chi_K = \gamma_2^K c_\sigma. \tag{3.12}$$

Upon moving into the glass state by increasing the positive σ, the cage effect becomes more efficient. This leads to a stiffening of the dynamics upon cooling, reflected by an increase of ω_K and χ_K. Measuring ω_K or χ_K, for example by shifting the $\log \chi''$ against $\log \omega$ curves on top of a master curve, yields t_σ or c_σ. Both quantities determine σ and allow one to identify the critical point T_c by extrapolation to $\sigma = 0$, equation (1.3), as was demonstrated in [22, 23].

The described stiffening of the cage-effect dominated dynamics is demonstrated by the spectra 7–9 in figure 2. The difference between the concave $\log \chi''$ against $\log \omega$ curve in the liquid and the convex curve in the glass within the described high-frequency window is a rather drastic one. It allows one to discriminate the $\sigma < -\sigma_0$ from the $\sigma > \sigma_0$ states at one glance on raw data of the spectra. Thereby one gets a first estimation of T_c within an accuracy of ± 20 K, as can be seen from the CKN examples in [23].

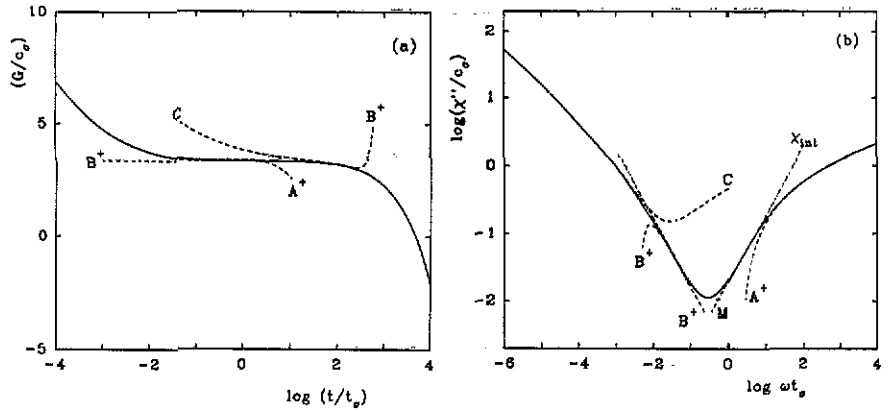

Figure 7. The same as figure 6 for $\lambda = 0.91$ and $\sigma/\sigma_0 = +7.2$.

3.2.3. Relaxation within the transition regime. For the transition region, where σ is small compared to σ_0, one can find the solution

$$G(t) = \xi c_\delta (t/t_\delta \xi^2)^{-a} \left(1 + \sum_l A_l (t/t_\delta \xi^2)^{l(1+2a)}\right) \qquad |\sigma| \ll \sigma_0. \tag{3.13}$$

Here

$$A_1 = -\frac{1}{2[\Gamma(1-a)\Gamma(a+2) - \lambda]} \tag{3.14}$$

and the other coefficients are given by (A7). The positive parameter $\xi = \xi(\sigma, \delta)$ varies smoothly with control parameters, it is constant on a scaling line: $\xi(\sigma, \delta) = \xi(\hat{\sigma}, \hat{\delta})$. The solution describes the dynamics for $\bar{t} \leqslant t \leqslant t_\delta$, as shown in figures 8($a$) and 9($a$). For shorter times and $\sigma \neq 0$ the expansions (3.8) or (3.11) apply. For $\sigma = 0$ the solution (3.13) has to extend the critical decay (2.3), i.e. $\xi(\sigma = 0, \delta) = 1$. In this case (3.13) provides the short-time expansion of g in (1.10). Therefore ξ remains of order unity also for $0 < |\sigma| \ll \sigma_0$. The solution (3.13) continues (3.8) or (3.11) with very good matching for $t \approx \bar{t}$, as exemplified in figures 8 and 9. For $\xi = 1$ the radius of convergence is again found to be strongly λ dependent: $r = 1.9$ for $\lambda = 0.74$ and $r = 0.59$ for $\lambda = 0.91$, estimated for $l = 100$.

The correlator (3.13) differs from glass behaviour by not showing a plateau, and from liquid dynamics by exhibiting the inflection point t_i of the $G(t)$ against $\log t$ graph not near the zero of the correlator but rather at $G(t_i) \approx \chi_\infty(\sigma = \sigma_0)$, compare figures 8($a$) and 9($a$). The susceptibility spectrum follows the critical law (2.3) with decreasing frequency much closer than described above for $|\sigma| \gg \sigma_0$. This comes about because the correction to the σ-independent leading term, which is proportional to $(\omega t_0)^a$, varies like $(\omega t_\sigma)^{-a}$ for $|\sigma| \gg \sigma_0$ but like $(\omega t_\delta)^{-1-a}$ for $|\sigma| \ll \sigma_0$. The latter term decreases much faster than the former with increasing frequency. The result (3.13) extends the spectrum just to the minimum position $\omega_{\min}$. If one would fit the spectrum for $\omega > \omega_{\min}$ by (3.8) or (3.11), the necessary suppression of the above-mentioned $(\omega t_\sigma)^{-a}$ correction terms would force one to place the minimum or the knee to frequency values much below $\omega_{\min}$. This is shown

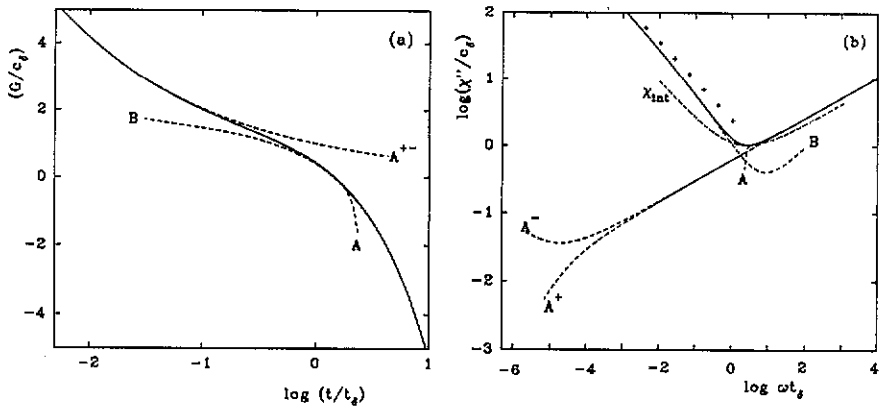

Figure 8. Correlator $G(t)$ and loss spectrum $\chi''(\omega)$ within the transition region for $\lambda = 0.74$ and $\sigma/\sigma_0 = \pm 5.210^{-3}$. The broken curves are the series expansions described in the text and the chain curve is the interpolation (3.17). The curves $A^{\pm}$ refer to $\sigma/\sigma_0 = \pm 5.210^{-3}$. The crosses denote the von Schweidler law $\chi'' \propto 1/\omega^b$.

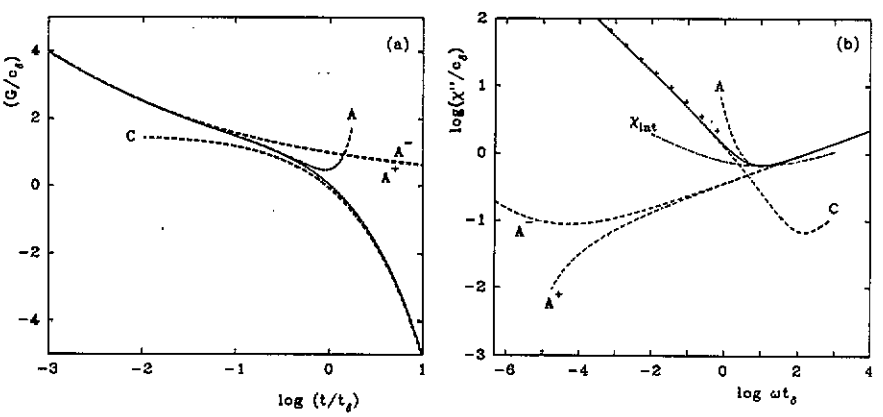

Figure 9. The same as figure 8 for $\lambda = 0.91$ and $\sigma/\sigma_0 = 5.210^{-3}$. $A^{\pm}$ refer to $\sigma/\sigma_0 = \pm 5.210^{-3}$.

by the fit curves $A^{\pm}$ in figures 8(b) and 9(b). Closely following the linear relation $\log \chi''(\omega) = a \log \omega +$ constant until the minimum is the most remarkable qualitative difference of the susceptibility spectrum in the transition region as opposed to that in the liquid. This is evident for curve 4 and 5 in figure 2. It is also apparent in the raw data shown in [23] for CKN at $T \approx 100°$ C; an observation which allows in that case to estimate T_c within $\pm 15°$ C.

3.3. β-minimum dynamics

The critical decay law (2.3) yields the sublinearly varying critical susceptibility spectrum (A8) within the high-frequency part of the β-relaxation window. The spectrum matches the microscopic excitation band at some frequency $\omega_{mic} \approx 1/t_0$. If one denotes the spectral intensity $\chi''(\omega = \omega_{mic}) = \chi_{mic}$, one can write the critical

spectrum as $\chi''_{cr}(\omega) = \chi_{mic}(\omega/\omega_{mic})^a$. A major prediction of the MCT is that the susceptibility spectrum below the microscopic band is strongly enhanced over the expected white noise background $\chi''_0(\omega) = \chi_{mic}(\omega/\omega_{mic})$. Because $a < 0.4$, one indeed finds for $\omega \ll \omega_{mic}$ that $\chi''_{cr}(\omega) \gg \chi''_0(\omega)$. The α peak is located at some frequency $1/\tau_\alpha$ outside the β region. It produces, with its high-frequency wing for $\omega\tau_\alpha \gg 1$, a susceptibility spectrum that decreases with increasing ω. Thus there appears a spectral minimum at $\omega = \omega_{min}$, where the spectral intensity $\chi''(\omega_{min}) = \chi_{min}$ is strongly enhanced over the white noise background. This holds, unless there is some mechanism of suppressing the critical spectrum. The β-relaxation theory describes a part of the high-frequency α-peak wing, thereby establishing a close link between α and β relaxation. The spectral minimum is the most outstanding feature of the β-relaxation dynamics. It will be shown that the spectral shape near the minimum and the scaling of the parameters ω_{min} and χ_{min} with variations of T are characteristically different for the three regions $\sigma \ll -\sigma_0$, $|\sigma| \ll \sigma_0$ and $\sigma \gg \sigma_0$ introduced above.

3.3.1. The β minimum for the liquid region. Again we consider the case $\sigma \ll -\sigma_0$. If $t_\sigma < t \ll \tilde{t}$, the hopping term can be neglected. Then series (A9) is the appropriate solution. Noting the von Schweidler term and its leading correction only one gets

$$G(t) = -B^- c_\sigma \left(\frac{t}{t_\sigma}\right)^b \left[1 - \frac{B_1^-}{(B^-)^2}\left(\frac{t}{t_\sigma}\right)^{-2b}\right] \tag{3.15}$$

with

$$B_1^- = \frac{1}{2[\Gamma(1+b)\Gamma(1-b) - \lambda]}. \tag{3.16}$$

These formulae are merely the long-time expansions of the scaling law of the simple version of the MCT (1.5) and (1.8). The constant B^- is tabulated as a function of λ in [9]. The result (3.15) matches (3.8) very well for $t \approx t_\sigma$, as shown in figures 4(*a*) and 5(*a*). It continues the convex $G(t)$ against $\log t$ graph to longer times exceeding t_σ. Similarly, the susceptibility spectrum is continued on the left part of the minimum. The scaling properties of the minimum are noted in (3.10). Upon cooling the cage effect becomes more efficient. This slows down the dynamics as reflected by the decrease of ω_{min}, χ_{min} upon approaching the transition region from the high temperature side.

The minimum is formed by the crossover from the von Schweidler fractal (A11) to the critical fractal (A8). The spectrum is stretched over several decades and exhibits the large enhancement over the white noise background, discussed above. Let us note for later reference that the β minimum of the liquid is described well by the handy interpolation formula

$$\frac{\chi''_{int}}{\chi_{min}} = \frac{1}{a+b}\left[b\left(\frac{\omega}{\omega_{min}}\right)^a + a\left(\frac{\omega}{\omega_{min}}\right)^{-b}\right]. \tag{3.17}$$

This is exemplified by the chain curves in figures 4(*b*) and 5(*b*). The series (A9) is semiconvergent only [9], and can merely be used to evaluate $G(t)$ for large times asymptotically. This means that matching can in general not be improved by extending (3.15).

3.3.2. The β minimum for the glass region. For positive separation parameters, i.e. $T < T_c$, a solution of (2.2) is provided by the series

$$G_\alpha(t) = \chi_\infty \Big(1 + \sum_l B_l^+ (t/\bar{t})^l\Big). \tag{3.18}$$

The parameters σ and δ enter χ_∞ and $\bar{t}$ via (1.7*b*) and (3.5). The coefficients B_l^+ are σ–δ-independent functions of λ; $B_1^+ = -1/2$ and the other terms follow from (A14). This function can be considered as the α-process contribution to the dynamics within the β-relaxation window. The solution $G_\alpha(t)$ of the scaling equation (2.2) is not identical with the β correlator, since it does not exhibit the initial condition (2.3). Therefore let us write

$$G(t) = G_\alpha(t) + G_\beta(t) \tag{3.19}$$

where $G_\beta(t)$ shall be viewed as the proper part of the β process. For very small times, the function $G_\beta(t)$ has to agree with the critical correlator. Since $G_\alpha(t \leqslant t_\sigma \ll \bar{t}) = \chi_\infty$ whenever $\sigma \gg \sigma_0$, one finds $G_\beta(t)$ to agree with the short-time solution (3.8) up to the subtraction term χ_∞:

$$G_\beta(t) = c_\sigma g_+ (t/t_\sigma) - \chi_\infty \qquad t \leqslant t_\sigma. \tag{3.20}$$

Let us anticipate that $G_\beta(t)$ decreases to zero with increasing time, so that one can define the waiting-time moments

$$M_n(\sigma, \delta t_0) = \frac{1}{t_0^{n+1}} \int_0^\infty t^n G_\beta(t)\,\mathrm{d}t \qquad n = 0, 1, \ldots. \tag{3.21*a*}$$

Since $G_\alpha(t)$ obeys the same scaling laws (2.4) as the full correlator $G(t)$, this is true also for $G_\beta(t)$. Therefore

$$M_n(\sigma, \delta t_0) = \hat{M}_n \Omega^{a-1-n}. \tag{3.21*b*}$$

The moment M_n for $(\sigma, \delta t_0)$ on a scaling line through $(\hat{\sigma}, \hat{\delta})$ can be expressed by $\hat{M}_n = M_n(\hat{\sigma}, \hat{\delta})$ up to a scale factor. The Laplace transform of the correlator can be written as

$$G(z) = G_\alpha(z) + \mathrm{i}t_0 \sum_n (\mathrm{i}z t_0)^n M_n. \tag{3.21*c*}$$

Let us apply (3.21*b*) with $\Omega = |\sigma|^{1/2a}$. Using the scales of section 3.1 one finds $M_n(\sigma, \delta t_0) = (t_\sigma/t_0)^{n+1} c_\sigma \hat{M}_n(1, x)$ with $x = (\sigma_0/\sigma)^{(1+2a)/2a}$. Anticipating $\hat{M}_n(1, x)$ to be smooth in x for $x \to 0$, one gets the result

$$M_n t_0^{n+1} = t_\sigma^{n+1} c_\sigma \gamma_n \qquad \sigma \gg \sigma_0. \tag{3.22}$$

The γ_n can be evaluated as moments of $(g_+ - 1/\sqrt{1-\lambda})$ from (1.5) and (1.7). The power series in (3.21*c*) is useful only for $|z t_\sigma| \ll 1$. For vanishing hopping rate δ,

the α tail is trivial: $G_\alpha(t) = \chi_\infty$. Thus there must exist a scale $\omega_{\min}$, which vanishes for $\delta \to 0$ and specifies the onset of deviation of $G_\alpha(t)$ from the plateau value

$$G(t) = \chi_\infty \qquad t_\sigma \ll t \ll \omega_{\min}^{-1}. \tag{3.23}$$

Combining the preceding three equations one derives for the β susceptibility for $\omega_{\min} \ll \omega \leqslant t_\sigma^{-1}$

$$\chi(\omega) = [\chi_\infty - c_\sigma(\omega t_\sigma)^2\gamma_1 + \ldots] + ic_\sigma(\omega t_\sigma)[\gamma_0 - (\omega t_\sigma)^2\gamma_2 + \ldots]. \tag{3.24}$$

In section 3.2.2 it was shown that the correlator tends to arrest at χ_∞ for $t \approx t_\sigma$. Equation (3.23) shows that it continues to do so up to the currently unspecified larger time $\omega_{\min}^{-1}$, as exemplified in figures 6(a) and 7(a). The susceptibility spectrum $\chi''(\omega)$ continues the σ-dependent knee, discussed in section 3.2.2, as shown in figures 6(b) and 7(b). In leading order the spectrum is a white noise spectrum:

$$\chi''(\omega_{\min} \ll \omega \ll t_\sigma^{-1}) = M_0(\omega t_0) \qquad M_0 t_0 = c_\sigma t_\sigma \gamma_0. \tag{3.25a}$$

The reactive part of the susceptibility is a constant in leading order:

$$\chi'(\omega_{\min} \ll \omega \ll t_\sigma^{-1}) = \chi_\infty. \tag{3.25b}$$

Equations (3.25) imply that within the specified window the α-peak tail contribution to the spectrum can be neglected compared to the proper β spectrum. However, there is a non-trivial contribution to the reactive part χ_∞. It can be measured in principle, for example as the reactive part of the elastic modulus. It determines the high-frequency sound velocity in the window, where α-relaxation dispersion is as negligible as β-relaxation contributions. Kramers–Kronig relations connect χ_∞ with spectral integrals. With (1.1) one finds

$$\frac{2}{\pi}\int \Phi_X''(\omega)\,\mathrm{d}\omega = f_X^c + h_X\chi_\infty \tag{3.26a}$$

$$\frac{2}{\pi}\int \chi_X''(\omega)\,\mathrm{d}\ln\omega = f_X^c + h_X\chi_\infty. \tag{3.26b}$$

The first integral has to be extended over the window $\omega \leqslant \omega_{\min}$ and the second over $\ln\omega \leqslant \ln\omega_{\min}$. The frequency $\omega_{\min}$ defines naturally the upper end of the α peak. The RHS of (3.26) is the α-peak area. The quantity $h_X\chi_\infty$ is thus identified as the temperature-dependent contribution to the α-peak intensity. This is a further link between α- and β-relaxation established by the MCT. The temperature dependence is singular, since (1.3) and (1.7b) imply $\chi_\infty \propto \sqrt{\sigma} \propto \sqrt{T_c - T}$. Measuring the α-peak area for $\sigma \gg \sigma_0$ yields the separation parameter and therefore by extrapolation the critical temperature, as shown in [12–14].

For times exceeding $\omega_{\min}^{-1}$, the proper β process dies out. The series (3.18) can be used efficiently up to order $\tilde{t}$, and so

$$G(t) = G_\alpha(t) \qquad \omega_{\min}^{-1} \ll t \ll \tilde{t}. \tag{3.27}$$

The correlator $G_\alpha(t)$ describes, within the specified t range, the onset of the cage decay as enforced by hopping effects. This is shown in figures 6(a) and 7(a). The

corresponding susceptibility is given by the Laplace transform of (3.18). Since the regular contributions due to G_β can be neglected for small $z = \omega + i0$, one finds

$$\chi(z) = \chi_\infty\left(-1 - \sum_l l! B_l^+ (-iz\tilde{t})^{-l}\right) \qquad \tilde{t}^{-1} < |z| \ll \omega_{\min}. \quad (3.28)$$

The highest-frequency part of the α process follows a stochastic dynamical pattern as described, for example, by a Debye law. In particular, the absorptive part exhibits the regular decay:

$$\chi''(\tilde{t}^{-1} \ll \omega \ll \omega_{\min}) = M_0'/\omega \qquad M_0' = \chi_\infty/2\tilde{t}. \quad (3.29)$$

This is shown in figures 6(*b*) and 7(*b*).

Formulae (3.24) and (3.28) describe the high- and low-frequency parts respectively of the β minimum within the glass, hence the notation for the relevant scale $\omega_{\min}$. The derived asymptotic formulae (3.24) and (3.28) do not match well for $\omega \approx \omega_{\min}$, cf figures 6(*b*) and 7(*b*). An obvious interpolation between the two asymptotic parts (3.25*a*) and (3.29) is provided by $\chi''_{\text{int}} = M_0\omega + M_0'\omega^{-1}$. This leads to an analogue of (3.17):

$$\frac{\chi''_{\text{int}}(\omega)}{\chi_{\min}} = \frac{1}{2}\left[\left(\frac{\omega}{\omega_{\min}}\right) + \left(\frac{\omega_{\min}}{\omega}\right)\right]. \quad (3.30)$$

The chain curves in figures 6(*b*) and 7(*b*) demonstrate that this expression works quite well. Substitution of the explicit expressions for M_0, M_0' yields for the minimum parameters

$$\omega_{\min} = \gamma_1^g/t_g \qquad \chi_{\min} = \gamma_2^g c_\sigma\sqrt{t_\sigma/\tilde{t}} = \gamma_2^g\sqrt{\delta t_0}|\sigma|^{-1/4a}. \quad (3.31)$$

Here t_g is given in (3.6) and $\gamma_1^g = 1/\sqrt{2\gamma_0\sqrt{1-\lambda}}$, $\gamma_2^g = \sqrt{\gamma_0/\sqrt{1-\lambda}}$ are expressed in terms of the spectral weights γ_0 of the glass master functions g_+ in (1.5), which are tabulated in [9].

Within the glass the β minimum is formed because hopping effects suppress the critical spectrum. The spectral shape is utterly different from that found in the liquid. There is no stretching, but a crossover from stochastic spectral decay (3.29) to white noise (3.25*a*). Moving into the glass by increasing σ, the system becomes stiffer and therefore $\omega_{\min}$ increases upon cooling for fixed hopping rate (δt_0). This is the same effect, discussed above for the spectral knee in (3.12). Similarly, if the rate δt_0 becomes bigger, the hopping effects can dominate for larger frequencies and so $\omega_{\min}$ rises with δt_0. Upon cooling δt_0 is expected to decrease [8]. This effect might partly compensate the mentioned increase of $\omega_{\min}$, a situation exemplified in figure 2 by the evolution from state 6 to 7. The decrease of δ might even overcompensate the stiffening as exemplified in figure 2 for state 9 relative to state 8. On the other hand, an increase of σ implies a decrease of $\chi_{\min}$. Upon moving into the glass the spectral intensity due to the sluggish motion near the critical point gets suppressed. Lowering the hopping rate further reduces the intensity $\chi_{\min}$. It would be very helpful for a judgment of the relevance concerning the present theory to test the predictions on the β minimum for $T < T_c$ by experiment. For CKN the interesting window would

extend 2–3 decades below 10 GHz, as can be inferred from [23]. The window is outside of the spectrometer range used for the light-scattering experiment in [23], but it is accessible by modern dielectric loss spectrometers. Due to the factorization property (1.1), both experiments test the same β dynamics. The predictions refer to a minimum in a broad background and therefore the experimental difficulties will be connected with signal-against-noise problems.

3.3.3. The β minimum for the transition region. A solution for $|\sigma| \ll \sigma_0$ is searched for that extends the short-time expansion (3.13) to $t \gg t_\delta$. The series (A12) and (A15) are candidates. The former can be used for $\Delta\lambda < 0$, since only for $b > 1/2$ is the series asymptotic for $t \to \infty$. Because $c < 1/2$ one can use (A15) as a large-time expansion for $\Delta\lambda > 0$. Replacing B_0 in (A12) by $B = B_0(\delta)^{-1/2} t_\delta^{b-1/2}$ and C_0 in (A15) by $B = C_0 t_\delta$, one gets

$$G(t) = -Bc_\delta \left(\frac{t}{t_\delta}\right)^b \left[1 + \sum_l \frac{B_l}{B^{2l}} \left(\frac{t}{t_\delta}\right)^{l(1-2b)}\right] \qquad b > \tfrac{1}{2} \tag{3.32a}$$

$$G(t) = -(\Delta\lambda)^{-1/2} c_\delta \left(\frac{t}{t_\delta}\right)^{1/2} \left[1 + \sum_l C_l \left(B\frac{t}{t_\delta}\right)^{l(c-\frac{1}{2})}\right] \qquad b < \tfrac{1}{2}. \tag{3.32b}$$

The parameter B is constant on a scaling line. For $\sigma = 0$ the expansion thus found provides the large-time asymptotics of the master function g in (1.10):

$$g(\hat{t}) = -B\hat{t}^b \left(1 + \sum_{l=1}^{l_0} \frac{B_l}{B^{2l}} \hat{t}^{l(1-2b)}\right) \qquad b > \tfrac{1}{2} \tag{3.33a}$$

$$g(\hat{t}) = -(\Delta\lambda)^{-1/2} \hat{t}^{1/2} \left(1 + \sum_{l=1}^{l_0} C_l (B\hat{t})^{l(c-\frac{1}{2})}\right) \qquad b < \tfrac{1}{2}. \tag{3.33b}$$

As explained in the last paragraph of section 3.3.1, the summation should be extended to the smallest value $l = l_0$, for which $b - l(2b-1)$ or $\frac{1}{2} - l(\frac{1}{2} - c)$ is negative. For example in figures 8 and 9 one gets $l_0 = 8$ and 3 respectively. The figures show that the series do not match nicely with the short-time expansion (3.13).

The correlators (3.32) describe the initial part of the α process, where $G(t) < 0$. The corresponding susceptibility spectrum is the high-frequency α-peak tail, cf figures 8 and 9. The dynamics is controlled by the hopping effect. The stretching of the relaxation is not as strong as within the liquid. This is reflected by the lower bound $\frac{1}{2}$ for the von Schweidler exponent. Furthermore, the $\log \chi''$ against $\log \omega$ curve is steeper near the minimum than given by the von Schweidler law. The spectrum, which forms the low-frequency wing of the β minimum, falls below the von Schweidler asymptote, shown in crosses in figures 8(b) and 9(b).

As in the liquid region, the β minimum in the transition range is obtained as a crossover between two fractals specified by a and b or $\frac{1}{2}$ respectively. This is a qualitative difference to that predicted for the glass. But, as in the glass, the crossover from one side of the minimum in the $\log \chi''$ against $\log \omega$ curve to the other is rather sharp; only one decade in figures 8(b) and 9(b). This is the qualitative difference to the spectral shape of the liquid. This difference is demonstrated most clearly by the

failure of the fit formula (3.17) as shown by the chain curves in figures 8(*b*) and 9(*b*). The scaling law (1.10) implies the σ-insensitive minimum parameters

$$\omega_{\min} = \gamma_1^{\mathrm{T}}/t_\delta \qquad \chi_{\min} = \gamma_2^{\mathrm{T}} c_\delta . \tag{3.34}$$

With increasing hopping rate δt_0 the spectrum increases, thereby shifting $\omega_{\min}$ to larger values. The frequency range for the critical decay is largest for $\sigma = 0$, as is obvious from figure 3 and as is exemplified by curves 4 and 5 in figure 2. A measurement of the spectrum in the transition regime would be the most sensitive means to fix the exponent parameter λ and the value for the rate δt_0 for $T = T_c$. Determination of the spectral shape on a three-decade window would provide a severe test of the present theory. One knows from [23] that the relevant dynamical window for CKN extends from 10 MHz to 10 GHz.

3.4. Very long-time dynamics

For times exceeding $\tilde{t}$ and t_δ the hopping term δt in the scaling equation (2.2) dominates the solution. The corresponding dynamical regime is described by the series (A12) and (A15) for $\Delta\lambda < 0$ or $\Delta\lambda > 0$ respectively. The regime is shared by the liquid, glass and transition region and should be considered as an extension of the latter, cf figure 3. The results (3.32) hold for sufficiently large times not only for $\sigma \ll \sigma_0$ but for all σ. The σ dependence enters via the parameter B only. Let us consider the details for glass and liquid separately. The term B_0 in (A12) shall be replaced by $\xi = B_0/(\sqrt{\delta}\tilde{t}^{(1-2b)/2})$. This is equivalent to writing $B = \xi(\tilde{t}/t_\delta)^{(1-2b)/2}$ in (3.32*a*) and yields

$$G(t) = -\xi\sqrt{1-\lambda}\chi_\infty(t/\tilde{t})^b\left(1 + \sum(B_l/\xi^{2l})(t/\tilde{t})^{l(1-2b)}\right) \qquad b > \tfrac{1}{2}. \tag{3.35a}$$

Similarly one writes $\xi = 1/\sqrt{C_0\tilde{t}}$ in (A15). This is equivalent to the substitution $\xi = (t_\delta/B\tilde{t})^{1/2}$ in (3.32*b*) and leads to

$$G(t) = -\sqrt{(1-\lambda)/\Delta\lambda}\chi_\infty(t/\tilde{t})^{1/2}\left(1 + \sum C_l(t/\tilde{t}\xi^2)^{l(c-\frac{1}{2})}\right) \qquad b < \tfrac{1}{2}. \tag{3.35b}$$

The parameter $\xi = \xi(\sigma,\delta) = \xi(\hat{\sigma},\hat{\delta})$ is constant on scaling lines. Hence one shows as usual that it is independent of control parameters deep in the glass $\sigma \gg \sigma_0$. The results scale like $G_\alpha(t)$ as studied in equations (3.18) and (3.27). Hence (3.35) continues the hopping induced decay of the cages, whose onset was discussed above in 3.2.2. There is good matching of the present results with $G_\alpha(t)$ for $t \approx \tilde{t}$, as shown in figures 6(*a*) and 7(*a*). The susceptibility spectrum equivalent to (3.35) is the low-frequency end of the β regime. It describes fractal decay again, as given in leading order by the von Schweidler law with exponents $b > \frac{1}{2}$ or $b = \frac{1}{2}$. Hence the α-peak wing exhibits a knee whose parameters sensitively depend on σ and δ via

$$\omega_{\mathrm{K}}^\alpha = \gamma_1^\alpha/\tilde{t} \qquad \chi_{\mathrm{K}}^\alpha = \gamma_2^\alpha\sqrt{\sigma}. \tag{3.36}$$

This knee marks a crossover from fractal α decay for $\omega \ll \omega_{\mathrm{K}}^\alpha$ to stochastic decay for $\omega \gg \omega_{\mathrm{K}}^\alpha$, as shown in figures 6(*b*) and 7(*b*). Notice that χ_{K}^α scales like the

α-peak intensity. Measurements of σ as the α-peak area are therefore not falsified, if the frequency cutoff in the integrals (3.26) is placed somewhere in the interval $\omega_K^a < \omega < \omega_{min}$ instead of at the minimum. Shifting the system into the glass by increasing σ decreases ω_K^a. The left part of the stochastic β-minimum increases thereby, as shown by the curves 7–9 in figure 2. Measurements of the regular variation of the knee position $\omega_K \propto \sigma$ or of the correlator zero $G(t_z) = 0$, $t_z \propto \sigma$, would be relevant tests of the present theory.

The long-time relaxation of the liquid, $\sigma \ll -\sigma_0$, is handled as above, albeit only if $b > \frac{1}{2}$. In this case the long-time expansion (3.32a) or (3.35a) can easily be rewritten, for example by using $B_0^2 = \xi^2 \delta(t_\sigma)^{1-2b}$ in (A12). This matching parameter ξ can be chosen such, that matching with (3.15) is established for $t \approx \bar{t}$, as shown in figure 4. Since the leading term in (3.15) has the same exponent b as in (A12), the two series describe so closely the same von Schweidler decay pattern that no particular anomaly for $t \approx \bar{t}$ or $\omega \approx \bar{t}^{-1}$ can be detected in figures 4(a) or 4(b).

For $b < \frac{1}{2}$ again (A12) shall be used, where B_0 is replaced by some other coefficient $\xi = B_0 t_\sigma^b / \sqrt{|\sigma|}$. The series is

$$G(t) = -\xi c_\sigma (t/t_\sigma)^b \left(1 + \sum (B_l/\xi^{2l})(t/t_c)^{(1-2b)l}\right) \tag{3.37}$$

where the scale t_c, equation (3.7), obeys the condition $t_c/\bar{t} \gg 1$ for $\sigma \ll -\sigma_0$. The leading term exhibits the same scaling as the one in (3.15). Good matching between these formulae is possible for $t \approx \bar{t}$, as shown in figure 5. Equation (3.37) extends the initial part of the α process, as described by (3.15), to times of order t_c. No particular anomaly in the dynamics is apparent for $t \approx \bar{t}$ or $\omega \approx 1/\bar{t}$. The series (3.37) cannot be used for times exceeding t_c, since $(1 - 2b) > 0$. For $t \approx t_c$ there occurs a crossover to a law like (3.35b) as shown in figure 5(b). With the choice $\xi = 1/\sqrt{C_0 t_c}$ in (A15) the expansion runs

$$G(t) = -\sqrt{|\sigma|/(\lambda - \lambda_0)}(t/\bar{t})^{1/2}\left(1 + \sum C_l (t/(t_c \xi^2))^{l(c-\frac{1}{2})}\right). \tag{3.38}$$

For $\omega = 1/t_c$ the α-peak tail exhibits an anomaly, but a different one from what was found for the α peak in the glass. With increasing frequency the von Schweidler decay $\chi'' \propto \omega^{-1/2}$ crosses over to an even stronger stretching $\chi'' \propto \omega^{-b}$ with $b < \frac{1}{2}$.

4. The liquid-to-glass crossover

In section 3 the shapes of the β correlators and of the susceptibility spectra were discussed. They were characterized by various scales. The latter had been introduced in an *ad hoc* manner and they were related to measurable quantities only in limiting cases. In this section the liquid-to-glass crossover shall be characterized by various scales to be identified as measurable features of the spectra. Let us remember the timescale t_δ, the correlation scale c_δ and the separation scale σ_0, induced by the hopping rate δt_0 via the formulae (3.2) and (3.4). They are connected elementarily by $\sigma_0 = (t_0/t_\delta)^{2a} = c_\delta^2$. Applying (2.4) with $\Omega = 1/t_\delta$ one gets

$$G(t) = c_\delta g(t/t_\delta, \sigma/\sigma_0, \hat{\delta} = 1) = c_\delta \hat{G}(t/t_\delta, \sigma/\sigma_0) \tag{4.1a}$$

$$\chi(\omega) = c_\delta \chi(\omega t_\delta, \sigma/\sigma_0, \hat{\delta} = 1) = c_\delta \hat{\chi}(\omega t_\delta, \sigma/\sigma_0) \tag{4.1b}$$

where the master functions $\hat{G}$ and $\hat{\chi}$ are specified by λ. In practical applications the precise connection of the relevant control parameters σ and δ with the physical control parameter T is not known. But these functions are smooth; δ is positive throughout and σ defines T_c by its zero as specified in (1.3). Figure 10 comprises the contents of the scaling equation (2.2) for the exponent parameter $\lambda = 0.91$. It exhibits $\hat{G}$ against $\log(t/t_\delta)$, $\log(\hat{\chi}'')$ and $\hat{\chi}'$ against $\log(\omega t_\delta)$ for a representative set of σ and constant $\delta t_0 = 1$. The examples characterizing the liquid, transition and glass regimes, explained in figures 5, 7 and 9 above, are shown as full curves.

The most obvious parameters specifying the scales of the relaxation process are the position of the susceptibility minimum $\omega_{\min}$ and the spectral intensity for this frequency $\chi_{\min} = \chi''(\omega_{\min})$. Because of (4.1*b*) there are two crossover functions $f_1(x), f_2(x)$ so that

$$\omega_{\min} = f_1(\sigma/\sigma_0)/t_\delta \qquad \chi_{\min} = f_2(\sigma/\sigma_0)c_\delta. \tag{4.2a}$$

The functions $f_{1,2}$ and similar functions below are independent of control parameters σ and δ. They are completely given by λ. From (3.10) one finds for the asymptotics specifying the ideal liquid state:

$$f_1(x \ll -1) = \gamma_1^{\mathrm{L}}|x|^{1/2a} \qquad f_2(x \ll -1) = \gamma_2^{\mathrm{L}}|x|^{1/2}. \tag{4.2b}$$

From (3.31) and (3.6) one derives the asymptotics within the glass state:

$$f_1(x \gg 1) = \gamma_1^{\mathrm{g}}|x|^{(1-2a)/4a} \qquad f_2(x \gg 1) = \gamma_2^{\mathrm{g}}|x|^{-1/4a}. \tag{4.2c}$$

The values of the functions for zero separation parameter have been introduced in (3.34):

$$f_1(x = 0) = \gamma_1^{\mathrm{T}} \qquad f_2(x = 0) = \gamma_2^{\mathrm{T}}. \tag{4.2d}$$

The upper two parts in figure 11 exhibit $(\omega_{\min} t_0)^{2a}$ and $\chi_{\min}^2$ against separation parameter σ. The full curve represents the result for $\sigma_0 = 1$ and hence the master functions f_1^{2a} and f_2^2 respectively. The broken curves are the asymptotes (4.2*b*) and (4.2*c*). The results for other σ_0 are found by rescaling according to (4.2*a*). This is demonstrated by the two chain curves. For $\sigma_0 \to 0$ the curves approach the asymptotes on the liquid side. These asymptotes are the result of the simple version of the MCT, dealing with the ideal freezing of the liquid. In the limit $\delta t_0 \to 0$ the functions converge towards zero for $\sigma > 0$. Notice that measurements of either diagram for a given temperature-independent δt_0 would yield $\sigma(T)$ and hence the critical temperature T_c. Let us combine the results to a third crossover function connected with the minimum:

$$\omega_{\min} t_0/\chi_{\min} = \sigma_0^{(1-a)/2a} f_3(\sigma/\sigma_0). \tag{4.3}$$

Since $f_3 = f_1/f_2$ one derives the asymptotes from (4.2*b*) and (4.2*c*). The defined combination approaches δ-independent asymptotes for the liquid $\sigma \ll -\sigma_0$ as well as for the glass $\sigma \gg \sigma_0$, which are proportional to $\sigma^{(1-a)/2a}$. Figure 11(*c*) shows this crossover function. Due to the insensitivity to temperature variations of δt_0 this plot is suggested for an identification of T_c from below and from above T_c.

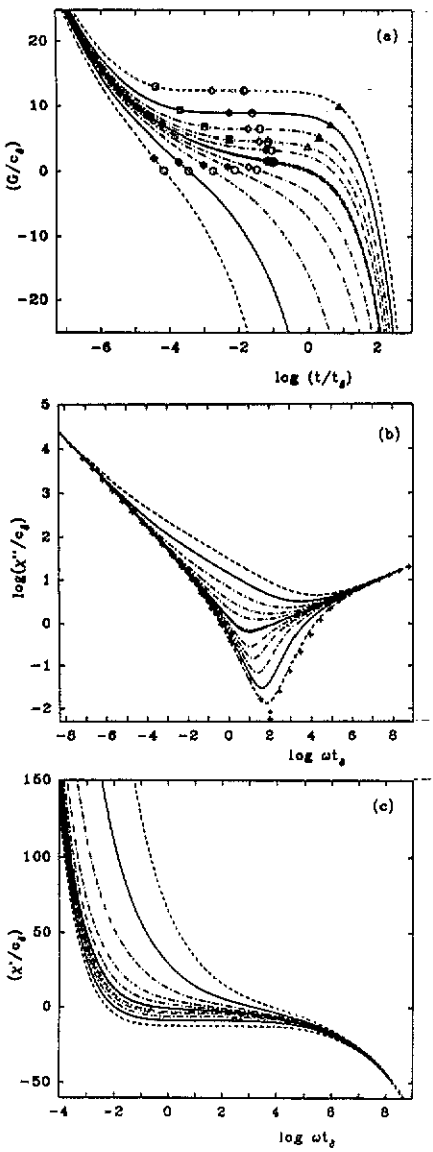

Figure 10. β correlators G as a function of $\log t$ and β susceptibilities $\chi'+i\chi''$ as a function of $\log\omega$ for exponent parameter $\lambda = 0.91$ and hopping rate $\delta t_0 = 1$. From below to above the curves in (a) and from above to below the curves in (b) and (c) refer to $\sigma = -13.9,\ -7.2,\ -3.7,\ -1.9,\ -1.0,\ -7.2\times10^{-2},\ \mp5.2\times10^{-3},\ 7.2\times10^{-2},\ 1.0,\ 1.9,\ 3.7,\ 7.2,\ 13.9$. The three full curves refer to the parameters discussed in figures 5, 7 and 9 respectively. In (a) the symbols from left to right respectively mark: ω_K^{-1}, t_i, ω_{min}^{-1} and $(\omega_K^{\alpha})^{-1}$. The crosses in (b) exhibit the interpolations (4.4).

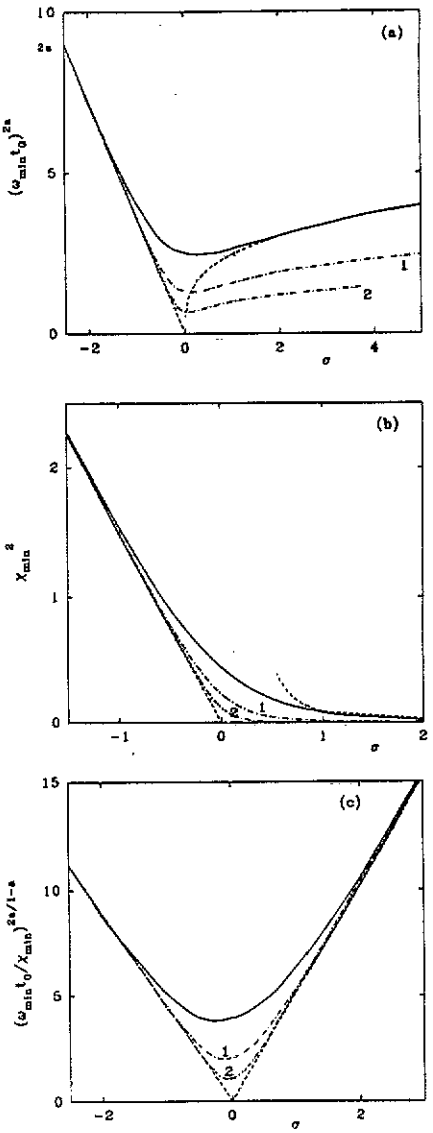

Figure 11. Quantities specifying the susceptibility minimum as function of the separation parameter σ, see text. The open circles are numerical results for $\delta t_0 = 1$ and the chain curves 1 and 2 are rescaled for $\delta t_0 = 10^{-1}$ and 10^{-2} respectively. The broken curves are the various asymptotic laws derived in the text.

Within the glass the susceptibility spectrum exhibits two knees. A possibility to define in a practical manner the parameters of the high-frequency knee ω_K, χ_K discussed in 3.2.2 and of the low-frequency knee $\omega_K^\alpha, \chi_K^\alpha$ discussed in 3.4, is the use of interpolations for the data in the neighbourhood of the knees. For the low-frequency knee we propose

$$\chi_{\text{int}}^{K\alpha}(\omega) = 2\chi_K^\alpha/[(\omega/\omega_K^\alpha)^b + (\omega/\omega_K^\alpha)]. \tag{4.4a}$$

Here b has to be replaced by $\frac{1}{2}$ in case of $\lambda > \lambda_0$. For the high-frequency knee one can use

$$\chi_{\text{int}}^{K}(\omega) = 2\chi_K/[(\omega_K/\omega)^a + (\omega_K/\omega)]. \tag{4.4b}$$

Instead of the interpolation (4.4b) it seems more promising to study a plot of $\chi''(\omega)/\sqrt{\omega}$. Due to $a < 0.4$ this plot results in a maximum at ω_K. The crosses in figure 10(b) demonstrate that the interpolations (4.4) are quite good for $\sigma/\sigma_0 = 13.9$ and define the knee parameters well. The preparation of the maximum at ω_K leads to comparable quality in determining ω_K and χ_K. Each knee is described by the two crossover functions

$$\omega_K = g_1(\sigma/\sigma_0)/t_\delta \qquad \chi_K = g_2(\sigma/\sigma_0)c_\delta \tag{4.5}$$

$$\omega_K^\alpha = g_1^\alpha(\sigma/\sigma_0)/t_\delta \qquad \chi_K^\alpha = g_2^\alpha(\sigma/\sigma_0)c_\delta. \tag{4.6}$$

Notice that these functions are defined only for $\sigma/\sigma_0 > x^* > 0$ or $\sigma/\sigma_0 > x_\alpha^* > 0$ respectively, since there are no knees in the liquid. For $\lambda = 0.91$ one finds $x^* \approx x_\alpha^* \approx 1.2$. From (3.12) one finds for the asymptotes for the high-frequency knee

$$g_1(x \gg 1) = \gamma_1^K |x|^{1/2a} \qquad g_2(x \gg 1) = \gamma_2^K |x|^{1/2}. \tag{4.7}$$

From (3.36) one finds the asymptotes for the α-peak knee:

$$g_1^\alpha(x \gg 1) = \gamma_1^\alpha |x|^{-1} \qquad g_2^\alpha(x \gg 1) = \gamma_2^\alpha |x|^{1/2}. \tag{4.8}$$

For $\lambda = 0.91$ the master functions follow the asymptotes (4.7) and (4.8) very well. Identification of ω_K and χ_K therefore is a good method to determine T_c from the low-temperature side.

Within the liquid β dynamics for $b < \frac{1}{2}$ one finds a crossover between the two von Schweidler laws referring to exponents b and $\frac{1}{2}$ respectively. The crossover can again be described by some interpolation formula. In section 5 it will become clear that α-relaxation corrections in general mask this feature of the β dynamics.

In figure 12 the various scales defined as obvious features of the $\log \chi''$ against $\log \omega$ diagrams are exhibited. This figure, as opposed to the schematic diagram shown as figure 3, demonstrates the crossover dynamics in quantitative detail. Together with the discussion of section 3 it exhibits the full contents of the scaling equation (2.2). Let us emphasize that the identified scales do not show up so clearly in the $G(t)$ against $\log t$ or χ' against $\log \omega$ diagrams, as can be inferred from figure 10. The only obvious scales suggested by the latter two quantities are the zeros: $G(t_z) = 0$ or $\chi'(\omega_z) = 0$. But these numbers are not directly measurable. Accessible to

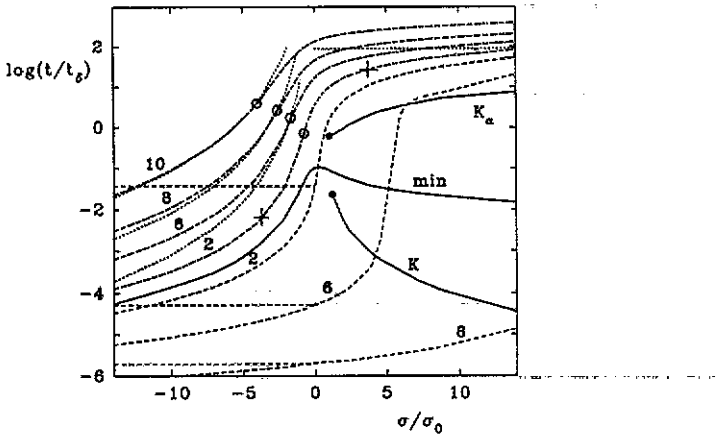

Figure 12. The various timescales calculated as function of σ for $\lambda = 0.91$. The full curves denoted by min, K and K_α are the inverse of the frequencies specifying the position of the minimum, the high frequency knee and the low-frequency knee in the susceptibility spectrum respectively. The broken curves are the short timescale t_s, defined in (5.1) and t_0 for $\delta t_0 = 10^{-2}$, 10^{-6}, 10^{-8}. The chain curves with lables 2, 6, 8, 10 denote the α scale t_α, defined in (5.6) for $\delta t_0 = 10^{-2}$, 10^{-6}, 10^{-8} and 10^{-10} respectively. Crosses on the $\delta t_0 = 10^{-2}$ curve mark the values of σ/σ_0 where $\sigma = \pm 1$. Dots on the chain curves mark the places where $t_\alpha = \tilde{t}$. The asymptote (5.8a) for t_α is shown as the dotted curve for the three values of $\delta t_0 = 10^{-6}$, 10^{-8} and 10^{-10}. The asymptote (5.10b) for t_α, denoted by a horizontal line, corresponds to $\delta t_0 = 10^{-10}$.

experiment is the full correlator $\Phi_X(t)$ or the full reactive part of the susceptibility χ'_X. These quantities differ from the one displayed in figure 10 by constants f_X^c and χ_X^c respectively, equations (1.1a) and (1.1b). But these constants are not easily accessible. Uncertainties in these numbers enter as uncertainties of t_z or ω_z.

Some of the experimental tests of the MCT predictions dealt with the determination of the α-peak area f_X or the high-frequency response χ_X^∞. Within the simple version of the MCT, treating a model of an ideal transition $\delta t_0 = 0$, these concepts are well defined mathematically. We could not invent a completely satisfactory definition of these concepts within the present theory so that the quantities are directly accessible by experiment. To propose measurable quantities which are as close as possible to the concepts of the idealized liquid-to-glass transition picture, we proceed as follows. By

$$\tilde{f}_X = \Phi_X(t_i) \tag{4.9a}$$

an effective Debye–Waller factor or Edwards–Anderson parameter for variables X shall be defined. Here t_i is the inflection point of the $\Phi(t)$ against $\log t$ curve. Because of (1.1a) one gets the prediction

$$\tilde{f}_X = f_X^c + h_X \Delta\tilde{f}. \tag{4.9b}$$

Here $\Delta\tilde{f}$ is the part of $\tilde{f}_X$ that varies rapidly near the glass transition singularity. It is given as $\Delta\tilde{f} = G(t_i)$ and deep in the glass it is the plateau value of the β correlator, which is exhibited for $\omega_K^{-1} \ll t \ll (\omega_K^\alpha)^{-1}$, cf figure 10($a$). From (4.1$a$) one obtains a scaling law expressing the crossover in terms of a master function h:

$\Delta\tilde{f} = c_\delta h(\sigma/\sigma_0)$. From (1.5) and (1.7*b*) one derives δ-independent asymptotes within the liquid or the glass:

$$\Delta\tilde{f}(\sigma \ll -\sigma_0) = \gamma_i\sqrt{|\sigma|} \qquad \Delta\tilde{f}(\sigma \gg \sigma_0) = \sqrt{|\sigma|}/\sqrt{1-\lambda}. \quad (4.10)$$

Here the number $\gamma_i = g_-(t_i/t_\sigma)$ is small but not zero. If it was zero, then by definition (4.9) $\tilde{f}_X$ would be identical to f_X^c in the liquid. Figure 13 displays the master function h for $\delta t_0 = 1$ and the asymptotes of the ideal transition scenario. The curve exhibits the smooth crossover as caused by hopping effects. The data analysis in [13] applied concepts close to the above prescription and the reported results indicate a rather small value of δt_0 for polybutadien.

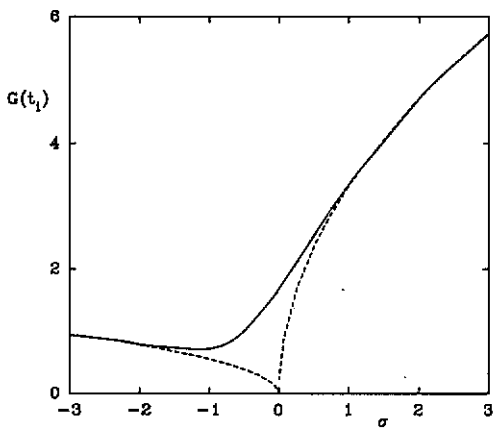

Figure 13. Effective non-ergodicity parameter $\Delta\tilde{f} = G(t_i)$ for $\delta t_0 = 1$. The broken curves are the square root asymptotes specified in the text.

The high-frequency tail of the α peak is identical to the low-frequency part of the β process. Therefore any theoretical discussion of the stiffness of the system in the regime $\omega\tau_\alpha \gg 1$ requires an understanding of the β processes. A natural limit of the α-peak process, which is directly measurable, is given by the minimum of the susceptibility spectrum, $\omega_{\min}$. By

$$\tilde{\chi}_X^\infty = \chi'_X(\omega = \omega_{\min}) \quad (4.11a)$$

an effective high-frequency susceptibility shall be defined, which generalizes the corresponding concepts of the simple version of the MCT. From (1.1*b*) one gets

$$\tilde{\chi}_X^\infty = \chi_X^c + h_X\tilde{\chi}_\infty^\alpha. \quad (4.11b)$$

Here $\tilde{\chi}_\infty^\alpha = \chi'(\omega_{min})$ is that part of $\tilde{\chi}_X^\infty$ that varies rapidly if the control parameter approaches the glass transition singularity $(\sigma, \delta) \to 0$. As above one finds the crossover as a scaling law $\tilde{\chi}_\infty^\alpha = c_\delta h^\alpha(\sigma/\sigma_0)$, with

$$\tilde{\chi}_\infty^\alpha(\sigma \ll -\sigma_0) = \gamma_i^\alpha\sqrt{|\sigma|} \qquad \tilde{\chi}_\infty^\alpha(\sigma \gg \sigma_0) = \sqrt{|\sigma|}/\sqrt{1-\lambda}. \quad (4.12)$$

Within the glass one finds the square root asymptotes given by the results of the ideal transition scenario, equation (1.7*b*). Here formulae (4.9*a*) and (4.11*a*) lead to the same result. Again in the liquid $\tilde{\chi}_X^{\infty}$ differs from χ_X^c due to the small γ_i^{α} only. Numerically it is found for $\lambda = 0.91$ that the master curve h^{α} differs from h only slightly. In [25] a high-frequency acoustic modulus M_{∞} was determined by a rather involved least-square fitting analysis of Brillouin scattering data. The data were discussed in relation to the MCT. However, we are unable to decide whether such a fitting procedure corresponds to the above suggestion of determining M_{∞}. This especially holds in cases $T > T_c$ where α and β processes are not clearly separated.

5. The β relaxation regime

The β relaxation regime is limited to small values for the separation parameter σ and the hopping rate δt_0. It is an asymptotic expansion near the glass transition singularity $(\sigma, \delta t_0) \to (0,0)$ dealing with correlators $\Phi_X(t)$ close to the corresponding non-ergodicity parameter f_X^c. The time has to be sufficiently large in order to eliminate short-time transient motion and corrections to the β- scaling equation. But it also has to be shorter than the scale specifying the α process. In this section the limits of the β regime shall be considered in more detail. Within a specific model the corrections can be calculated with the β correlator $G(t)$ as input. For small $(\sigma, \delta t_0)$ and close to the critical non-ergodicity parameter the corrections are of order $G(t)^2$ in general. There are further contributions proportional to σ and δt which are independent of $G(t)$. The corrections to the leading asymptotic are not universal and therefore in the following only order of magnitude estimations can be presented.

A short-time cutoff t_s can be defined by requiring the correlator $\Phi_X(t) = f_X^c + h_X^c G(t)$ to be close to the non-ergodic value:

$$G(t_s) = 1 \qquad G(t) < 1 \quad \text{for } t > t_s. \tag{5.1}$$

The X dependence of this definition has been omitted. Elimination of the short-time transient motion further requires $t > t_0$, i.e. for $(\sigma, \delta t_0) \to (0,0)$ β dynamics will be observed for

$$t > t_s \quad \text{and } t > t_0. \tag{5.2}$$

Equation (5.1) can be solved leading to

$$t_s = t_\delta f_s(\sigma/\sigma_0, \sigma_0) \tag{5.3}$$

where f_s depends explicitly on σ and δ, i.e. it does not obey a one-parameter scaling law. In the liquid case for $\sigma \ll -\sigma_0$ and if $|\sigma| \ll 1$ the correlator G_{cr} can be used in (5.1) to get $t_s \approx t_0$. In the glass $\sigma \gg \sigma_0$ the plateau value $\chi_\infty = \sqrt{\sigma/(1-\lambda)}$ becomes larger than unity leading to $t_s > \bar{t} > t_{min}$. For such high values of σ, where the plateau moves out of the specified region around f_X^c, the mentioned correction terms, which are independent of $G(t)$, are in general not small even if $G(t) < 1$. Figure 12 shows t_s and t_0 for different values of δt_0. A maximal value δ^* for the hoping rate δ can be obtained by requiring the minimum in $\chi''(\omega)$ to be in the β window:

$$t_{min} \geqslant \max(t_s, t_0) \quad \text{for} \delta < \delta^*. \tag{5.4}$$

From figure 12 it can be seen that equations (5.1) and (5.2) lead to $\delta^* t_0 \approx 10^{-2}$ for $a = 0.2$.

If δ is close to the maximal value δ^*, the separation parameter σ is restricted to the transition regime

$$|\sigma| < \sigma_0 \quad \text{for} \quad \delta \approx \delta^*. \tag{5.5}$$

In this case only the relaxation patterns, discussed in figures 8 and 9 can be described by the present theory. The interesting evolution of the liquid β spectrum into the transition regime upon increasingly negative σ towards $-\sigma_0$ and the evolution out of the transition regime upon increasing σ above σ_0 lies beyond the range of applicability of the present theory if $\delta \approx \delta^*$. In this case the hopping effects are so efficient that they mask the results expected within the simple version of the MCT, dealing with an idealized liquid-to-glass transition.

If δ is sufficiently smaller than the maximum value δ^*, $|\sigma|$ is allowed to exceed σ_0 and the idealized cage effects can be observed. In the liquid state requiring separation of microscopic and β timescales lead to $\sigma > -|\sigma_-^*|$. In the glassy state the region of validity is restricted by the condition that the time t_{min} should exceed t_s. This gives an upper cutoff $\sigma < |\sigma_+^*|$. In general $|\sigma_-^*| \neq |\sigma_+^*|$ and both depend strongly on δt_0. The restriction $|\sigma| \ll 1$ however may not be neglected, i.e. $|\sigma_+^*|, |\sigma_-^*| \ll 1$ has to be hold.

The β correlator diverges for large times, too. On the other hand, the complete correlator is bounded $|\Phi_X(t)| \leqslant \Phi_X(t = 0)$. Thus a natural large-time cutoff t_α appears by the requirement $\Phi_X(t_\alpha) = f_X + h_X G(t_\alpha) = -\Phi_X(t = 0)$. For times comparable to t_α the α-decay process, which is not treated within the present theory, depends on X. Ignoring this X dependence one gets for $(\sigma, \delta) \to (0, 0)$ an estimation for the specified scale characterizing the onset of the α corrections to β dynamics from the equation

$$G(t_\alpha) = -1. \tag{5.6}$$

From (4.1a) one finds

$$t_\alpha = f_\alpha(\sigma/\sigma_0, \sigma_0) t_\delta. \tag{5.7a}$$

Here the function $f_\alpha(x, y)$ of the two variables $x = \sigma/\sigma_0$ and $y = \sigma_0$ does not exhibit homogeneity properties. It follows via (4.1a) as the solution of the equation

$$\hat{G}(f_\alpha(x, y), x)\sqrt{y} = -1. \tag{5.7b}$$

The chain curves in figure 12 exhibit the results for three values of δt_0.

Within the liquid state one can use the von Schweidler law (3.15) for the β correlator in order to derive

$$t_\alpha = t_0/[(B^-)^{1/b}|\sigma|^\gamma] \qquad \gamma = \frac{1}{2a} + \frac{1}{2b} \qquad -1 \ll \sigma \ll -\sigma_0. \tag{5.8a}$$

Using the von Schweidler asymptote requires

$$t_\sigma \ll t_\alpha. \tag{5.8b}$$

This condition is ensured by the requirement $|\sigma| \ll c^-(\lambda) < 1$, where $c^-(\lambda)$ denotes a constant depending on λ only. Violation of (5.8*b*) implies that the α relaxation and the β process merge and are close to the microscopic transient motion. This merging cannot be described by the simple power law (5.8*a*). In figure 12 the asymptote (5.8*a*) is shown for three values for δt_0. For $\delta t_0 = 10^{-6}$ the corrections of (3.15) to the von Schweidler asymptote are not negligible due to σ being too large. The corrections determining $c^-(\lambda)$ depend strongly on λ and are large for the case $\lambda = 0.91$. The used von Schweidler law ignores the influence of hopping events and this requires

$$t_\alpha \ll \tilde{t} \quad \text{or} \quad -\sigma \gg \sigma_\alpha = [\delta t_0/(B^-)^{1/b}]^{2ab/(a+b+2ab)}. \tag{5.8c}$$

If t_α approaches $\tilde{t}$, the hopping effects modify the σ-dependent prefactor in (3.15) and this alters the power law variation (5.8*a*). The corresponding points, where $t_\alpha = \tilde{t}$ are marked by dots in figure 12.

Within the transition region $|\sigma| \ll \sigma_0$ one can use (3.32) to solve equation (5.6) for t_α. Due to having more than one divergent term in (3.32) for $\hat{t} \to \infty$ one can analytically find a solution only for $\delta t_0 \to 0$ also:

$$t_\alpha = t_\delta/(Bc_\delta)^{1/b} \qquad b > 1/2 \qquad |\sigma| \ll \sigma_0 \ll 1 \tag{5.9a}$$

$$t_\alpha = t_\delta(\Delta\lambda/c_\delta^2) \qquad b < 1/2 \qquad |\sigma| \ll \sigma_0 \ll 1. \tag{5.9b}$$

If $\delta \ll \delta^*$, one gets $t_\alpha \gg t_\delta$. For $\delta \to \delta^*$ the α, β and microscopic process merge so that the dynamics near the β minimum can no longer be described by the present theory.

For the glass state the equation (5.6) is solved with the dominant contributions from (3.35). Using only the leading von Schweidler asymptotes with $b > 1/2$ or $1/2$ leads to

$$t_\alpha = \tilde{t}/(\sqrt{\sigma}\xi)^{1/b} \qquad \text{for } b > 1/2 \tag{5.10a}$$

$$t_\alpha = (\Delta\lambda)/\delta \qquad \text{for } b < 1/2. \tag{5.10b}$$

The restriction $|\sigma| \ll c^+(\lambda) < 1$ or $t_\alpha \gg \tilde{t}$ has to be fulfilled for equation (5.10) to hold; see the discussion below (5.8*b*). Again the corrections are strongly λ dependent and determine the constant $c^+(\lambda)$. In the present case, $\lambda = 0.91$, the asymptote (5.10*b*) is not observed in figure 12. Since $c^+(\lambda) \ll c^-(\lambda)$ the corrections in (3.35*b*) even for $\delta t_0 = 10^{-10}$ do not decay sufficiently fast to open the window $\sigma_0 \ll \sigma \ll c^+(\lambda)$.

The relevance of the scale t_α for the theory of the α process itself is unclear at present. Only in the liquid case $\sigma \ll -\sigma_0$ close to the transition $|\sigma| \ll 1$ the α process is known to obey a scaling law $\Phi_X(t) = F_X^\alpha(t/\tau)$ and asymptotic matching in the von Schweidler regime gives [27]:

$$\tau = t_0\sigma^{-\gamma} \qquad \text{for } \sigma \ll -\sigma_0 \quad |\sigma| \ll 1. \tag{5.11}$$

6. Summary

The MCT suggests the β relaxation as an explanation for the anomalously large susceptibility spectra between the microscopic band and the α relaxation. A glass transition singularity is approached when undercooling a liquid. This causes a slowing down of the dynamics. At the singularity the separation parameter $\sigma \propto T_c - T$ vanishes, defining the liquid-to-glass crossover temperature T_c. Phonon-assisted hopping transport introduces one additional relevant parameter δ into the β-relaxation theory; $\delta \neq 0$ prevents the physical system from reaching the singularity. The MCT calculates the β relaxation for small σ and δ, i.e. for temperatures T close to T_c and for experimental systems where δ is small. In the specified mesoscopic frequency window various experimental techniques probe the same β-relaxation correlator $G(t)$ up to intensity prefactors. The microscopic structure of the glass forming system enters $G(t)$ via one parameter λ only. In the idealized MCT neglecting hopping transport two master functions $g_\pm$ describe liquid and glassy relaxation respectively. Phonon-assisted transport, i.e. δ, introduces a natural scale σ_0 for σ. Only for $|\sigma| \gg \sigma_0$ the results of the idealized MCT are recovered. In a transition region around T_c limited by $\sigma(T) = \pm\sigma_0$ hopping effects cannot be ignored and distort the spectra.

In the liquid for temperatures T above the transition region, i.e. $\sigma \ll -\sigma_0$, the one-parameter scaling law of the idealized MCT $\chi''(\omega) = c_\sigma \chi''_-(\omega/\omega_\sigma)$ applies to the spectra. The interpolation formula (3.17) well describes the broad crossover from the critical power law $(\omega/\omega_\sigma)^a$ to the von Schweidler $(\omega/\omega_\sigma)^{-b}$. The minimum position varies with the scaling frequency $\omega_\sigma \propto (T - T_c)^{(1/2a)}$.

When entering the transition region upon cooling, hopping effects first appear on the low-frequency wing of the β minimum. There the idealized theory falls below the spectrum. The corrections are due to the interplay of hopping and cage effects for $\omega \approx \tilde{\omega} = \delta/\sigma$. Moreover for $\lambda > \pi/4$ the exponent of the long-time limit changes from the von Schweidler b to $\frac{1}{2}$.

Within the transition region the δ-dominated susceptibility (1.10) exhibits a sharp transition from the critical to the von Schweidler law with exponent b or $\frac{1}{2}$ respectively. The critical law ω^a almost extends to the minimum frequency. The minimum position appears at a finite frequency proportional to ω_δ.

Upon further cooling a knee on the high-frequency wing of the minimum appears when T is below T_c, i.e $\sigma \gtrsim \sigma_0$. At this knee the spectrum falls below the critical law. A plot of $\chi''/\sqrt{\omega}$ against ω results in a maximum at ω_K, which scales with ω_σ. A prediction of the MCT is that this spectral feature becomes faster upon cooling. The full MCT predicts a minimum for $T < T_c$ and its complicated dependence on σ and δ. A low-frequency knee at $\omega_K^< \propto \tilde{\omega}$ appears additionally.

In the glass well below the transition region the idealized β-MCT describes the high-frequency wing of the spectrum. The high-frequency knee at $\omega_K \propto \omega_\sigma$ results from the crossover from the critical to a white noise spectrum ω^1. The white noise spectrum can only be observed if knee and minimum position are well separated. The glass minimum depends sensitively on σ and δ (3.31) and (3.6). It is caused by a change from a white noise to a Debye-like relaxation ω^{-1}. The temperature dependence of the minimum position is strongly influenced by temperature drifts in δ. At the low-frequency knee at $\omega_K^< \propto \tilde{\omega}$ the Debye-like spectrum bends over to the von Schweidler or $\omega^{-1/2}$ asymptote.

Due to the inclusion of hopping effects it is now possible to quantitatively test the

β relaxation close to T_c. Especially challenging are the results in the transition region and in the glass. The range of frequencies ω, where the present theory is predicted to apply, is largest for $T \approx T_c$.

Acknowledgments

We thank Professor H Z Cummins for many helpful discussions. We thank him and his co-workers also for the permission to study their results prior to publication.

Appendix A. Recursion relations

Seven power series can be identified that solve the scaling equation (2.2) in various regions of time and parameters (σ, δ). In this appendix the recursion relations for the coefficients α_l for these series will be derived. With two exponents u and v a solution shall be written as

$$G(t) = t^u \sum_{l=0,1,\ldots} \alpha_l t^{lv}. \tag{A1}$$

Substitution in (2.2) yields

$$\sigma - \delta t - t^{2u}[\alpha_0^2 \Gamma_{00}/\Gamma(1+2u)] - t^{2u+v}[2\alpha_0\alpha_1\Gamma_{01}/\Gamma(1+2u+v)] - \sum_{l=2,3,\ldots} [t^{2u+lv}/\Gamma(1+2u+lv)] \sum_{n=0}^{l} \Gamma_{nl-n}\alpha_n\alpha_{l-n} = 0. \tag{A2}$$

Here the following abbreviation is used:

$$\Gamma_{nm} = \Gamma(1+x_n)\Gamma(1+x_m) - \lambda\Gamma(1+x_n+x_m) \qquad x_l = u + lv. \tag{A3a}$$

The procedure consists of two steps. First, the four numbers u, v, α_0 and α_1 are chosen such that the third and fourth terms of (A2) cancels the first two terms. Second, requiring the remaining term in (A2) to vanish yields a recursion relation, expressing the α_l for $l \geqslant 2$ in terms of u, v, α_0, α_1. It is written as

$$\begin{aligned} &\alpha_0 = \alpha \qquad \alpha_l = \alpha a_l \qquad \text{for} \quad l \geqslant 1 \\ &a_l = [-1/2\Gamma_{0l}] \sum_{n=1}^{l-1} \Gamma_{nl-n} a_n a_{l-n}. \end{aligned} \tag{A3b}$$

Two series treat the short-time solution for $\delta = 0$ [9]. Choosing $u = -a$ one obtains $\Gamma_{00} = 0$ because of (1.2a). With $v = 2a$ and $\alpha_1 = \sigma/[2\alpha_0\Gamma_{01}]$ the desired cancellations are achieved. Equation (A3b) leads to $a_l = \sigma^l A_l^+/\alpha^{2l}$, where A_l^+ depends neither on σ nor on α. The result is for $\sigma \gtrless 0$:

$$G(t) = A^{\pm} t^{-a} \left(1 + \sum A_l^{\pm} [|\sigma|^{1/2} t^a / A^{\pm}]^{2l}\right). \tag{A4}$$

Here, and in the following, l sums are extended over $l = 1,2,\ldots$. The leading coefficient $A_1^{\pm}$ is given by (3.9), and the others follow with $A_l^- = (-1)^l A_l^+$ from (A3), where one has to identify

$$\alpha = A^+ \qquad a_l = A_l^+ \qquad x_l = -a + 2la. \tag{A5}$$

In order to ensure the proper asymptote (2.3) one has to choose $A^+ = A^- = t_0^a$. The result (A4) gets the form (3.8) or (3.11).

A third series provides the short-time expansion for $\sigma = 0$. One proceeds as above but has to choose $v = 1 + 2a$ and $\alpha_1 = -\delta/(2\alpha_0\Gamma_{01})$. The recursion relation leads to $a_l = \delta^l A_l/\alpha^{2l}$ with A_l being independent of δ and α. The result is

$$G(t) = At^{-a}\left(1 + \sum A_l[\delta t^{1+2a}/A^2]^l\right) \tag{A6}$$

with A_1 given by (3.14) and the other A_l derived from (A3) with

$$\alpha_0 = A \qquad a_l = A_l \qquad x_l = -a + 2la + l. \tag{A7}$$

From (1.9) one gets for the spectrum

$$\chi''(\omega) = \sin(\tfrac{1}{2}\pi a)\Gamma(1-a)A\omega^a + O(\omega^{-a}). \tag{A8}$$

For this expression to be positive for large frequencies one has to require $A > 0$. Let us replace A by a positive parameter ξ by writing $A = \xi^{1+2a} t_0^a$. Then (A6) gets the form (3.13). This choice introduces the appropriate timescale t_δ into (3.13). Furthermore one can easily convince oneself that $\xi(\sigma,\delta)$ obeys the simple scaling law $\xi(\sigma,\delta) = \xi(\hat{\sigma}\hat{\delta})$, i.e. it is a constant on a scaling line through $(\hat{\sigma}\hat{\delta})$. With this choice of A the series in (A6) sums up terms of the form $(t/t_\delta\xi^2)^{(1+2a)l}$. Leaving the scaling line $\sigma = \hat{\sigma} = 0$, where (A6) was derived, only requires replacing $\hat{t} = t/t_\delta$ by $\hat{t} = t/t_{sc}$ introduced in (3.1) and the claimed homogeneity of ξ follows from the central two parameter scaling law (2.4). Analogous reasoning applies throughout the paper whenever the zeroth coefficients A_0, B_0 and C_0 of the expansions of this appendix are rewritten with the help of some timescale and a $(\hat{\sigma},\hat{\delta})$-dependent matching parameter like ξ.

The trick used above was to enforce $\Gamma_{00} = 0$ by a proper choice of u. This can exploited also with $u = b$, because of (1.2b). Formulae for the new series are obtained from above by the change $a \to -b$. The analogue of (A4) is the fourth series of interest:

$$G(t) = -B_0^- t^b\left(1 + \sum B_l^-[\sigma/(B_0^- t^b)^2]^l\right) \tag{A9}$$

where A^- has been replaced by $-B_0^-$. This series will be applied only for $\sigma < -\sigma_0$, hence the notation. The coefficient B_1^- is noted in (3.16) and the others follow from (A3) with

$$-\alpha = B_0^- \qquad a_l = B_l^- \qquad x_l = b - 2lb. \tag{A10}$$

With (1.9b) one gets as the leading term the von Schweidler spectrum for the susceptibility:

$$\chi'' = \sin(\tfrac{1}{2}\pi b)\Gamma(1+b)(B_0^-)\omega^{-b}. \tag{A11}$$

Since this has to be positive, one finds $B_0^- > 0$. If one eliminates B_0^- in favour of a constant B^- by $B_0^- = (\sqrt{|\sigma|}/t_\sigma^b)B^-$, one gets equation (3.15).

The fifth series is the analogue of (A6), where $A \to -B_0$. Again $B_0 > 0$ is required:

$$G(t) = -B_0 t^b \left(1 + \sum B_l (\delta t^{1-2b}/B_0^2)^l\right). \tag{A12}$$

The first coefficient follows from (3.14) with $a \to -b$ and the others follow from (A3) with the translation list

$$-\alpha = B_0 \qquad a_l = B_l \qquad x_l = b + (1-2b)l. \tag{A13}$$

A sixth series is of particular interest since it solves (A2) for all parameter pairs $\sigma > 0, \delta \geqslant 0$. Let us use $u = 0$, $v = 1$. Then $\Gamma_{00} = \Gamma_{01} = (1-\lambda)$. Cancellation of the first four terms in (A2) can be achieved by $\alpha_0^2 = \sigma/(1-\lambda) = \chi_\infty^2$ and $\alpha_1 = -\delta/[2\alpha_0(1-\lambda)]$. The recursion relation (A3) yields $a_l = (\delta/\sigma)^l B_l^+$ with coefficients B_l^+ independent of σ and δ. The result is noted as (3.18), where $B_1^+ = 1/2$ and for $l \geqslant 2$:

$$B_l^+ = -\sum_{n=1}^{l-1} [(n!(l-n)!/l!) - \lambda] B_n^+ B_{l-n}^+ / [2(1-\lambda)]. \tag{A14}$$

Another solution is obtained by choosing $\alpha_0 = -\chi_\infty$. However, for $\delta \to 0$ this alternative would lead to arrest of the correlator at a non-ergodicity parameter $G(t \to \infty) = -\chi_\infty$, which is lower than the one implied by (3.19). This is not compatible with the general properties of the solution of the MCT equations [4]. Continuity in δ thus excludes the possibility of $\alpha_0 < 0$. Examining the B_l numerically for l up to 170 we found a strongly λ-dependent radius of convergence $|B_l|^{-1/l} \to r_\lambda$: $r = 0.55$ for $\lambda = 0.74$ and $r = 0.14$ for $\lambda = 0.91$.

The seventh series is found if one cancels the hopping term in (A2) against the third term of that equation by using $u = 1/2$. In this case $-\Gamma_{00} = \Delta\lambda$ from (1.11). Thus for $\Delta\lambda > 0$ and $\sigma = 0$ a solution is obtained as $G(t) = \alpha_0 t^{1/2}$, $\alpha_0 = -\sqrt{\delta/\Delta\lambda}$. As above the alternative with a positive α_0 has to be rejected. This special solution can be generalized to $\alpha_l \neq 0$ for $l \geqslant 1$, if one ensures $\Gamma_{01} = 0$ by choosing $v = c - 1/2$, with c given by (1.2c). The recursion relation implies $a_l = a_1^l C_l$ with coefficients C_l solely given by λ. The result is

$$G(t) = -\sqrt{\delta/\Delta\lambda}\, t^{1/2} \left(1 + \sum C_l [C_0 t]^{l(c-1/2)}\right) \qquad \Delta\lambda > 0. \tag{A15}$$

Here $C_1 = 1$ and the other coefficients follow from (A3) with

$$a_l = C_l \qquad x_l = 1/2 + l(c - 1/2). \tag{A16}$$

Appendix B. The long-time decay for $\lambda \to \pi/4$

The formulae derived in sections 3.3.3 and 3.4 become invalid if the exponent parameter λ approaches the critical value $\lambda_0 = \pi/4$. In this appendix the decay for very long times shall be considered for $\Delta = \lambda - \pi/4$ tending to zero. Remember, that it is sufficient to study the scaling equation (2.1) for $\sigma = 0$:

$$i\delta/z + \lambda z LT[G^2](z) + [z LT[G](z)]^2 = 0. \tag{B1}$$

For small Δ one can expand the equations (1.2b) and (1.2c) for the exponents b and c:

$$\Delta = -2\zeta(b - 1/2) + O(b - 1/2)^2 = \zeta(1/2 - c) + O(1/2 - c)^2 \tag{B2}$$

with $\zeta = \pi(2\ln 2 - 1)/4 \simeq 0.303$. Obviously the series (3.32b) and (3.35b) become meaningless for $\Delta \to 0$. To find a proper substitute we use an extension of the theory of slowly varying functions, invented in another context [26].

Let us write

$$F(t) = (t/t_0)^x f(u) \qquad u = \ln(t/t_1). \tag{B3a}$$

One finds the asymptotic expansion for the Laplace transform $F(z) = LT[F](z)$:

$$-zF(z) = (-izt_0)^{-x} \sum_{\nu=0,1,\ldots} \frac{1}{\nu!} \Gamma^{(\nu)}(1 + x) f^{(\nu)}(y) \qquad y = \ln[1/(-izt_1)]. \tag{B3b}$$

Here $\Gamma^{(\nu)}$ denotes the νth derivative of the gamma function. These formulae shall be applied for the β correlator with $x = 1/2$:

$$G(t) = -(t/t_0)^{1/2} l(u). \tag{B4}$$

The second term in (B1) is reformulated with $x = 1$, $f = l^2$ and the third one with $x = 1/2$, $f = l$. The result is an equation for the function l:

$$\delta t_0 - \Delta l^2 - 2\zeta l l' = O(\Delta l l', l' l', l l''). \tag{B5}$$

If the contribution on the RHS can be neglected compared to the LHS one readily solves the differential equation for l:

$$l(u) = [(\delta t_0/\Delta)(1 - e^{-\Delta u/\zeta})]^{1/2}. \tag{B6a}$$

This yields the desired solution in leading order:

$$G(t) = -[\delta t/\Delta]^{1/2}[1 - (t_1/t)^{\Delta/\zeta}]^{1/2}. \tag{B6b}$$

There appears a new timescale t_Δ for the dynamics, specifying the crossover from $|\Delta u/\zeta| \ll 1$ to $|\Delta u/\zeta| \gg 1$:

$$t_\Delta = t_1 e^{\zeta/\Delta}. \tag{B7}$$

One finds in particular

$$G(t) = -[\delta t \ln(t/t_1)/\zeta]^{1/2} \qquad t_1 \ll t \ll t_\Delta. \tag{B8}$$

This solution treats the long-time decay for $\lambda = \pi/4$. For $t \gg t_\Delta$ one can expand the second factor in (B6*b*) in order to recognize with (B2), that the closed formula for $G(t)$ is a summation of the series (3.35*b*) and (3.38).

In order to justify the concept of leading order, one has to determine the leading corrections. This is a straight forward extension of the discussion of (B5). Let us note the special result for $\Delta\lambda = 0$ only:

$$G(t) = -[\delta t \ln(t/t_1)/\zeta]^{1/2}[1 + C \ln\ln(t/t_1)/\ln(t/t_1)]. \tag{B9}$$

Here C is δ independently given by gamma functions.

In applications to discussions of the β decay on reasonable frequency windows, the logarithmic functions or the functions $(t_1/t)^{\Delta/\zeta}$ appear as constants that merely assure the correct matching.

References

[1] Wong J and Angell C A 1976 *Glass: Structure by Spectroscopy* (Basel: Dekker)
[2] Goldstein M 1969 *J. Chem. Phys.* **51** 3728
[3] Götze W and Sjögren L 1992 *Rep. Prog. Phys.* **55** 241
[4] Götze W 1991 *Liquids, Freezing and the Glass Transition* ed J P Hansen, D Levesque and J Zinn-Justin (Amsterdam: North-Holland) p 287
[5] Forster D 1975 *Hydrodynamic Fluctuations, Broken Symmetry, and Correlation Functions* (Reading: Benjamin)
[6] Palmer R G 1982 *Adv. Phys.* **31** 669
[7] Sjögren L 1990 *Z. Phys.* B **79** 5
[8] Götze W and Sjögren L 1988 *J. Phys. C: Solid State Phys.* **21** 3407
[9] Götze W 1990 *J. Phys.: Condens. Matter* **2** 8485
[10] Götze W and Sjögren L 1987 *Z. Phys.* B **65** 415
[11] Mezei F 1991 *Ber. Bunsenges. Phys. Chem.* **95** 1118
[12] Petry W, Bartsch E, Fujara F, Kiebel M, Sillescu H and Farago B 1991 *Z. Phys.* B **83** 175
[13] Frick B, Farago B and Richter D 1990 *Phys. Rev. Lett.* **64** 2921
[14] Börjesson L, Elmroth M and Torell L M 1990 *J. Chem. Phys.* **149** 209
[15] Sjögren L 1990 *Basic Features of the Glassy State* ed J Colmenero and A Alegria (Singapore: World Scientific) p 137
[16] Sjögren L 1991 *J. Phys.: Condensed Matter* **3** 5023
[17] Doster W, Cusack S and Petry W 1990 *Phys. Rev. Lett.* **65** 1080
[18] Van Megen W and Pusey P N 1991 *Phys. Rev.* A **43** 5429
[19] Götze W and Sjögren L 1991 *Phys. Rev.* A **43** 5442
[20] Barrat J L, Roux J N and Hansen J P 1990 *Chem. Phys.* **149** 197
[21] Fuchs M, Götze W, Hildebrand S and Latz A 1992 *Z. Phys.* B **87** 43
[22] Cummins H Z, Li G, Du W M, Chen X K, Tao N J and Sakai A 1992 *Proc. 1st Tohwa University Int. Symp., Fukuoka* in press
[23] Li G, Du W M, Chen X K, Cummins H Z and Tao N J 1992 *Phys. Rev.* A **45** 3867
[24] Mezei F, Knaak W and Farago B 1987 *Phys. Scri.* T **19** 363
[25] Elmroth M, Börjesson L and Torell L M 1992 *Phys. Rev. Lett* **68** 79
[26] Götze W and Sjögren L 1989 *J. Phys.: Condensed Matter* **1** 4203
[27] Götze W 1984 *Z. Phys.* B **56** 139